

Braiding non-ribbon surfaces and constructing broken fibrations on smooth 4-manifolds

A Dissertation Presented

by

Mark Clifford Hughes

to

The Graduate School

in Partial Fulfillment of the Requirements

for the Degree of

Doctor of Philosophy

in

Mathematics

Stony Brook University

August 2014

Stony Brook University

The Graduate School

Mark Clifford Hughes

We, the dissertation committee for the above candidate for the Doctor of Philosophy degree, hereby recommend acceptance of this dissertation.

Oleg Viro – Dissertation Advisor
Professor, Department of Mathematics

Dennis Sullivan – Chairperson of Defense
Professor, Department of Mathematics

Olga Plamenevskaya
Professor, Department of Mathematics

Martin Rocek
Professor, Department of Physics

This dissertation is accepted by the Graduate School.

Charles Taber
Dean of the Graduate School

Abstract of the Dissertation

**Braiding non-ribbon surfaces and constructing
broken fibrations on smooth 4-manifolds**

by

Mark Clifford Hughes

Doctor of Philosophy

in

Mathematics

Stony Brook University

2014

In this thesis we study various notions of surface braidings in 4-space, and their applications to the construction of singular fibrations on smooth oriented 4-manifolds. We define the notion of braided link cobordisms in $S^3 \times [0, 1]$, which generalize Viro's closed 2-braids in S^4 . We prove that via isotopy any properly embedded oriented surface $W \subset S^3 \times [0, 1]$ can be brought to this special position, and that the isotopy can be taken rel boundary when ∂W already consists of closed braids.

These surfaces are closely related to another notion of surface braiding in $D^2 \times D^2$, called braided surfaces with caps, which gener-

alize Rudolph's braided surfaces. We use these to construct broken Lefschetz fibrations on smooth 4-manifolds. We first consider the case when the 4-manifold X has connected non-empty boundary, and construct the desired fibration as the composition of a covering $X \rightarrow D^2 \times D^2$ branched along a singular braided surface with caps, with the projection map $\text{pr}_2 : D^2 \times D^2 \rightarrow D^2$. Proceeding in this way gives us the ability to specify the behavior of our fibration along ∂X . Broken Lefschetz fibrations on closed manifolds are then obtained by combining this result with a construction of Gay and Kirby. This allows us to reprove earlier existence results due to Akbulut and Karakurt, Baykur, and Lekili, giving a more concrete geometric approach to constructing these fibrations.

To Kimberly, Henry, Jane, and Dorothy.

Contents

List of Figures	viii
Acknowledgements	x
1 Introduction	1
1.1 Braiding surfaces in four dimensions	1
1.2 Braided surfaces and Lefschetz fibrations	2
1.3 Braided cobordisms and the Khovanov-Rozansky homology . .	4
1.4 Main results	6
1.5 Summary	9
2 Surface braidings in 4-space	11
2.1 Links as braid closures	11
2.2 Braided surfaces in $D^2 \times D^2$	12
2.3 Braided link cobordisms in $S^3 \times [0, 1]$	14
2.4 Braided cobordisms from braided surfaces	15
2.5 Braided surfaces with caps	17
2.6 Summary of surface braidings	19

3	Braiding link cobordisms	20
3.1	Movie presentations of braided cobordisms	20
3.2	Braiding around critical points	23
3.3	Braiding critical point free cobordisms	24
3.4	Geometric Markov moves for closed braids in \mathbb{R}^3	25
3.5	Threading construction	27
3.6	Braiding movie presentations without Reidemeister moves	29
3.7	Braiding movie presentations with Reidemeister moves	37
4	Singular fibrations on smooth 4-manifolds	42
4.1	Open book decompositions of 3-manifolds	42
4.2	Singular fibrations on 4-manifolds	43
4.3	Boundary conditions on fibrations	44
4.4	Near-symplectic manifolds and broken fibrations	45
4.5	Constructions of fibrations on closed 4-manifolds	47
4.6	The topology of broken Lefschetz fibrations	49
4.7	Replacing anti-Lefschetz critical points	55
5	Broken Lefschetz fibrations via branched coverings	59
5.1	Singular branched coverings	60
5.2	Constructing the branched coverings	61
5.3	Constructing the broken fibration	65
	Bibliography	78

List of Figures

2.1	Braided surface with caps	18
3.1	Braided movie presentation of a braided cobordism	22
3.2	Braiding saddle points	24
3.3	Cobordisms not isotopic rel boundary	25
3.4	Simple Markov equivalence	26
3.5	Trefoil as a closed braid given by a threading	28
3.6	Reidemeister-like moves involving the braid axis	33
3.7	Reidemeister-like move which does not lift to a braid isotopy .	34
3.8	Replacing bad Reidemeister-like moves of type III	34
3.9	Reidemeister-like moves of type II	35
3.10	Decomposing a simple Markov equivalence	37
3.11	Overpass choices in a neighborhood of type I and II moves . .	40
3.12	Threading near a Reidemeister move of type III	40
4.1	Vanishing cycle of Lefschetz critical point	50
4.2	Passing a round 1-handle singularity	51
4.3	Fibration on handles of index 0 and 1	52
4.4	Modifying fibration for fiberwise 2-handle attachment	52

4.5	Concave broken fibration on $S^2 \times D^2$	56
4.6	Replacing an anti-Lefschetz critical point	57
4.7	Surgery cycle in the fiber for Lekili's replacement	58
5.1	3-fold branched cover $\Sigma \rightarrow D^2$	63
5.2	3-dimensional branched covering moves	64
5.3	Loops c_α, c_β , and c_δ around critical values in D'	69
5.4	Braid monodromy around α , and associated braid twist arc . .	70
5.5	Braid monodromy around δ , and associated braid twist arc . .	70
5.6	Braid monodromy around β , and associated braid twist arc . .	70
5.7	Positive braid twist along and arc	71
5.8	Braid whose closure yields $B_G \cap (D \times C_{-1})$	72
5.9	Merging strands to give fold line	73
5.10	Branched covering $\phi : \Sigma_z \rightarrow D \times \{z\}$	74
5.11	$F \times D^2$ with additional handles	75
5.12	Handle structure on $S^2 \times D^2 \subset S^4$	76

Acknowledgements

I owe an enormous debt of gratitude to my wife Kim, for all of her love and support during the writing of this thesis. Thanks for being patient and understanding during the many hours I spent staring blankly of into space, trying to understand the details of this work. Thanks also to my children. Without you, this thesis would probably have been finished a lot sooner, but I would have had a lot less fun along the way. You were simultaneously a great motivating factor and a joyful distraction. Now that this is finished I will set at work trying to answer some of the many open questions Henry has posed, like whether ∞ is even or odd. Thanks also to my extended family, and especially my parents. You have been incredibly patient and supportive during this whole process, and are a big part of why this was possible.

This work, of course, would not have been possible without the help and guidance of my advisor, Professor Oleg Viro. He posed the original problem that inspired this work, and was instrumental in directing and helping me work through the many difficulties that arose along the way.

I am also grateful to many of the post-docs and my fellow graduate students at Stony Brook. Yury, Nathan, Chaya, Jonathan, Shane, Patricio, Ben, and Somnauth are just a few on this list. The math related discussions we had

helped answer many questions, while the non-math related discussions helped preserve my sanity. Thanks for your friendship and help along the way.

Chapter 1

Introduction

Two of the most useful and foundational results in knot theory and low-dimensional topology are the classical theorems of Alexander and Markov. These theorems allow us to carry out the development of knot theory entirely within the realm of braids and braid closures, where we can exploit either the algebraic structure of the braid group, the special position of a closed braid in S^3 , or the fact that braids with isotopic closures can be related by Markov moves. These results have been used in numerous applications, examples of which include the construction and categorification of quantum link invariants [14, 25, 33], the construction of open book decompositions on 3-manifolds [2], and studying the slice and ribbon genera of knots [41, 43].

1.1 Braiding surfaces in four dimensions

The notion of a closed braid as a specially positioned 1-dimensional submanifold of 3-dimensional space has been generalized by different authors to certain

classes of surfaces in 4-space. One such generalization is due to Rudolph [41], who considered surfaces $S \subset D^2 \times D^2$ on which the projection to the second factor $\text{pr}_2 : D^2 \times D^2 \rightarrow D^2$ restricts as branched coverings. This generalizes the classical notion of a (geometric) braid as a 1-dimensional submanifold of $D^2 \times [0, 1]$, on which the projection $\text{pr}_{[0,1]} : D^2 \times [0, 1] \rightarrow [0, 1]$ restricts as an ordinary covering. These surfaces are called *braided surfaces*, and are closely related to a similar notion due to Viro [46]. Rudolph showed that every orientable ribbon surface with boundary properly embedded in $D^2 \times D^2$ is isotopic to a braided surface. In this thesis we generalize these notions further, by defining *braided surfaces with caps*, and use them to construct fibration structures on smooth 4-manifolds.

Another approach to braiding surfaces is to try arranging the surface so that its level sets (with respect to some height function) are closed braids in some space. More precisely, we can consider properly embedded oriented surfaces $W \subset S^3 \times [0, 1]$, and try to isotope them so that the regular level sets $W \cap (S^3 \times \{t\})$ are all closed braids in $S^3 \times \{t\}$. We call these types of surfaces *braided link cobordisms*, and study them below. They can be related to braided surfaces with caps, by identifying $S^3 \times [0, 1]$ with a collar neighborhood of $\partial(D^2 \times D^2)$.

1.2 Braided surfaces and Lefschetz fibrations

Braided surfaces have found use in various applications, including finding obstructions to sliceness in knot theory [43], and the study of Stein fillings of contact 3-manifolds [36]. Here we outline another such application, due to

Loi and Piergallini, which uses Rudolph's surface braiding algorithm in the construction of Lefschetz fibrations on 4-dimensional 2-handlebodies (i.e. 4-manifolds admitting handle decompositions with no 3 or 4-handles). Lefschetz fibrations are closely related to symplectic 4-manifolds (see Section 4.4), and have been studied extensively in recent years.

In particular, suppose X is an oriented 4-manifold with a fixed handle decomposition that has no 3 or 4-handles. Then we can construct a covering $H : X \rightarrow D^2 \times D^2$ branched simply along an orientable ribbon surface S , which we can assume is a braided surface by Rudolph's algorithm. Then the composition $X \xrightarrow{H} D^2 \times D^2 \xrightarrow{\text{pr}_2} D^2$ is an achiral Lefschetz fibration, with a Lefschetz critical point (resp. anti-Lefschetz critical point) for each positive (resp. negative) branch point of $S \rightarrow D^2$. Thus if S has only positive branch points, we obtain a true Lefschetz fibration. In fact, Loi and Piergallini show that any sufficiently nice Lefschetz fibration over D^2 necessarily factors in this way.

Using these constructions, Loi and Piergallini also prove that for an oriented connected compact 4-manifold X with boundary, the existence of a Stein structure is equivalent to the existence of a Lefschetz fibration over D^2 with all vanishing cycles non-separating in the fiber. By considering the associated simple branched covering restricted to ∂X , it follows that a 3-manifold is Stein fillable if and only if it admits a positive open book decomposition.

Now suppose we start instead with a handlebody description of a 4-manifold X which has 3 and 4-handles. As noted above we can construct a branched covering of the 0,1, and 2-handles over $D^2 \times D^2$, branched along a ribbon surface. Once we try to extend this covering to the 3 and 4-handles how-

ever, the branch locus is no longer ribbon, and may additionally have cusp and node singularities. Rudolph’s algorithm does not extend to such surfaces, and hence any attempts to generalize the above branched covering methods require techniques for braiding more general surfaces. Our study of braided surfaces with caps, which we describe in Section 2.5, will provide an approach for generalizing these constructions.

1.3 Braided cobordisms and the triply-graded Khovanov-Rozansky homology

One potential application for braided cobordisms, and the author’s original motivation for this study, involves extending the link homology theories of Khovanov and Rozansky [32, 33] to surfaces. While we do not develop this here in any depth, we include a brief discussion of it as additional motivation for our study of braided cobordisms.

Starting with an oriented link diagram and integer $n \geq 2$, Khovanov and Rozansky [32] use matrix factorizations to construct a bigraded chain complex whose chain homotopy equivalence type is an invariant of the underlying link L . The homology of this complex is thus a link invariant, which we denote by $\mathcal{H}_n(L)$. It is bigraded, and from the graded Euler characteristic we can recover the sl_n -polynomial of L . The $n = 2$ case is equivalent [23] to Khovanov’s original categorification of the Jones polynomial described in [31].

Given an oriented smooth properly embedded surface $W \subset S^3 \times [0, 1]$ with boundary links $L_0 = W \cap (S^3 \times \{0\})$ and $L_1 = \overline{W \cap (S^3 \times \{1\})}$ (where

the overline indicates that we are reversing the orientation induced as the boundary of W), Khovanov and Rozansky's theory extends to give a map $\varphi_W : \mathcal{H}_n(L_0) \rightarrow \mathcal{H}_n(L_1)$. This map is an invariant of W up to isotopies fixing ∂W , and is defined as a composition of maps of the form $\mathcal{H}_n(L_t) \rightarrow \mathcal{H}_n(L_{t'})$, where L_t and $L_{t'}$ are nearby regular level sets of W .

Modifying the above approach, in [33] Khovanov and Rozansky defined a triply-graded link homology theory, which yields a triply-graded vector space $\mathcal{H}(L)$ for any oriented link L . This additional grading comes at some expense unfortunately, as the complex associated to a diagram is no longer invariant (up to chain homotopy equivalence) under all of the Reidemeister moves. This problem can be avoided however, by exclusively computing $\mathcal{H}(L)$ using diagrams of closed braid representatives of L . Indeed, the complex they associate to each link diagram is invariant (up to chain homotopy equivalence) under the braid-like Reidemeister moves.

Because of this extra braid restriction however, any hopes of a similar extension¹ of the triply-graded theory to surfaces would require that we first arrange $W \subset S^3 \times [0, 1]$ so that each regular level set $W \cap (S^3 \times \{t\})$ is a closed braid. Moreover, as above we would expect that the desired map would only be invariant under isotopies of W rel ∂W . Hence if ∂W already consisted of closed braids, we would need to be able to perform our braiding operations rel ∂W . Theorem 1.4.1 below provides a first step towards developing this approach.

¹It is known that Khovanov and Rozansky's triply-graded homology theory is not functorial. Indeed, $\mathcal{H}(U)$ is an infinite dimensional \mathbb{Q} -vector space, and hence it does not admit the structure of a Frobenius algebra. Thus we can expect at most a partial or restricted extension of this homology theory to surfaces.

1.4 Main results

We prove the following:

Theorem 1.4.1. *Let $W \subset S^3 \times [0, 1]$ be a smooth oriented properly embedded link cobordism. Then W is isotopic to a braided cobordism. If the boundary links of ∂W are already closed braids, then this isotopy can be chosen rel ∂W .*

Theorem 1.4.1 can be thought of as the cobordism analogue to the classical Alexander’s theorem, and will be proven in Chapter 3. Our construction will be similar to Kamada’s construction of the normal braid form of a surface link [30], which implies our result in the case that W is a closed surface. The bulk of the additional work here will be in carrying out the construction in a way that allows us to keep ∂W fixed during the required ambient isotopies. To do this, we make use of Morton’s diagram threading technique, which was introduced in his proof of the Markov theorem [39]. Our proof utilizes enhanced versions of the arguments contained in that proof. This boundary-fixing requirement is considered with an eye toward potential applications (see e.g. Section 1.3 and Chapter 5, as well as [24] which contains a construction that is not invariant under general isotopies of W).

Translating Theorem 1.4.1 to surfaces in $D^2 \times D^2$ gives us the following corollary:

Corollary 1.4.2. *Let S be a smooth oriented properly embedded surface in $D^2 \times D^2$. Then S is isotopic to a braided surface with caps. If ∂S is already a closed braid in $\partial(D^2 \times D^2)$, then the isotopy can be chosen rel ∂S .*

The techniques described in Section 1.2 can be generalized using Corol-

lary 1.4.2 along with results in the theory of 3-dimensional branched covers, due to Piergallini [40] and Montesinos [37]. This yields the following existence result, which we prove in Chapter 5 (where all the relevant terms will be defined):

Theorem 1.4.3. *Let X be a smooth oriented 4-manifold with connected nonempty boundary. Then we can construct a convex broken Lefschetz fibration $f : X \rightarrow D^2$, so that the restriction $f|_{\partial X} : \partial X \rightarrow D^2$ matches any specified open book decomposition with connected page and binding. Moreover, the following properties hold:*

1. *the images of the broken singularities can be arranged as a set of concentric circles parallel to ∂D^2 , with all Lefschetz singularities inside the innermost circle,*
2. *all fibers are connected,*
3. *the fiber genus increases by one for every broken singularity we pass as we move towards the center of D^2 ,*
4. *all vanishing cycles are nontrivial in the homology of the fiber F over $0 \in D^2$, and*
5. *f factors as $X \xrightarrow{H} D^2 \times D^2 \xrightarrow{\text{Pr}_2} D^2$, where H is a simple 4-fold covering branched along a braided surface with caps, and possibly cusp and node singularities.*

Note that after stabilization any open book decomposition can be assumed to have connected binding. We refer to a fibration as *factorizable* if it factors

through a simple covering branched along a braided surface with caps in $D^2 \times D^2$ with only cusp and node singularities as in Property 5 above.

By work of Auroux, Donaldson, and Katzarkov [4], broken Lefschetz fibrations share a close relationship with near-symplectic structures on 4-manifolds (see Section 4.4), and have been a subject of study in recent years. The literature contains a number of results proving the existence of various broken fibration structures on closed 4-manifolds [1, 5, 13, 16, 35], which we outline in Section 4.5. These techniques each involve either deep classification theorems from contact topology, or the modification of generic smooth functions around their critical points. Theorem 1.4.3 allows us to avoid the use of this machinery, and provides a more concrete geometric approach to the construction of broken Lefschetz fibrations. In particular, it allows us to prove the following theorem:

Theorem 1.4.4. *For any smooth oriented closed 4-manifold X , and any closed oriented connected surface $F \subset X$ with $[F]^2 = 0$, there exists a broken Lefschetz fibration $f : X \rightarrow S^2$ with all fibers connected, and with fiber F above the north pole. Furthermore,*

1. *all broken critical circles of f lie parallel to the equator,*
2. *all Lefschetz critical values of f lie in small neighborhood of south pole,*
3. *all vanishing cycles are nontrivial in the homology of the fiber over the south pole, and*
4. *the fiber genus increases by +1 for every singular circle we pass traveling south.*

Moreover, if there is an embedded sphere in X which intersects F transversely in a single point, then f factors as $X \xrightarrow{H} S^2 \times S^2 \xrightarrow{\text{pr}_2} S^2$, where H is a simple 4-fold covering branched along a surface with cusp and node singularities.

Theorem 1.4.4 is a slight strengthening of an existence result of Lekili [35], who proved the existence of a broken Lefschetz fibration satisfying properties 1-4. The branch locus $B_H \subset S^2 \times S^2$ of the covering H in Theorem 1.4.4 has the property that away from the cusp singularities, the critical points of the restriction of $\text{pr}_2 : S^2 \times S^2 \rightarrow S^2$ are all either positive branch points, or lie along the boundary of a cap of B_H with respect to $\text{pr}_2|_{B_H}$ (see Section 2.5).

It should be noted that constructions relating (broken) Lefschetz fibrations to branched coverings of surface bundles have been studied previously. Indeed, suppose that X admits a Lefschetz fibration whose vanishing cycles are non-separating and whose monodromy lies in the hyperelliptic mapping class group of the fiber. Then Fuller [15] and Siebert and Tian [45] proved independently that X admits a 2-fold covering of an S^2 -bundle over S^2 , branched along a surface. A similar result was proved by Hayano and Sato [20] for broken Lefschetz fibrations with fiber genus $g \geq 3$, and critical points which can be arranged in a specific configuration (so-called *simplified* broken Lefschetz fibrations introduced by Baykur [6]).

1.5 Summary

The remainder of this thesis will be organized as follows. In Chapter 2 we define various notions of surface braidings in $D^2 \times D^2$ and $S^3 \times [0, 1]$, as well as outline the relationships between them. In Chapter 3 we present diagrammatic

methods for studying 1-dimensional braids and surfaces in 4-space, before using them to prove Theorem 1.4.1. Chapter 4 contains a discussion of the different fibration structures on 3 and 4-manifolds which we will be interested in, as well as their connections to symplectic and near-symplectic topology. We also present some examples and constructions which will be needed in Chapter 5. Finally, in Chapter 5 we prove Theorem 1.4.3 by constructing a branched covering of our 4-manifold over $D^2 \times D^2$ with suitably braided branch locus. The proof of Theorem 1.4.4 is then obtained by combining this result with the constructions described in Chapter 4. We finish by showing that our construction applied to S^4 recovers the broken Lefschetz fibration originally described by Auroux, Donaldson, and Katzarkov [4].

Chapter 2

Surface braidings in 4-space

In this chapter we give precise definitions for many of the objects alluded to in Chapter 1, and set up much of the notation that will be needed in the rest of this thesis. The related notions of *braided surfaces*, *braided surfaces with caps*, and *braided cobordisms* will be defined, and we will explain how to pass between them.

2.1 Links as braid closures

Let $D^2 \subset \mathbb{C}$ be the unit disk, and $S^3 = \{(z, w) : |z|^2 + |w|^2 = 1\} \subset \mathbb{C}^2$ the unit 3-sphere. We set $T_1 = S^3 \cap \{z \leq \frac{1}{\sqrt{2}}\}$ and $T_2 = S^3 \cap \{w \leq \frac{1}{\sqrt{2}}\}$, and let $U = S^3 \cap \{w = 0\}$ (i.e. the core of T_2). We say that an oriented link L in S^3 is a *closed braid* if $L \subset S^3 \setminus U$, and $\arg(w)$ is strictly increasing as we traverse the components of L in the positively oriented direction. We call U the *axis* of the closed braid.

Note that T_1 and T_2 are both tori, and T_1 admits a natural product struc-

ture $T_1 \cong D^2 \times S^1$ induced by the maps $\rho : T_1 \rightarrow D^2$ given by $\rho(z, w) = \sqrt{2}z$, and $\rho' : T_1 \rightarrow S^1$ given by $\rho'(z, w) = \arg(w)$. If we fix this induced product structure $T_1 \cong D^2 \times S^1$, then ρ and ρ' are just projection onto the first and second factors respectively, which we will write as pr_1 and pr_2 . We fix a similar product structure on $T_2 \cong S^1 \times D^2$. Then a link $L \subset T_1$ is a closed braid if and only if $\text{pr}_2|_L : L \rightarrow S^1$ is a covering map. We call the degree of the covering map $\text{pr}_2|_L$ the *index* of the closed braid L .

Alexander's theorem then says that any oriented link in S^3 is isotopic to a closed braid. Markov's theorem says that any two closed braids which are isotopic as links can be joined by a sequence of isotopies through closed braids, as well as stabilization and destabilizations moves which increase and decrease the braid index respectively.

2.2 Braided surfaces in $D^2 \times D^2$

Rudolph defined a *braided surface* [41] to be a smooth properly embedded oriented surface $S \subset D^2 \times D^2$ on which the projection to the second factor $\text{pr}_2 : D^2 \times D^2 \rightarrow D^2$ restricts as a simple branched covering¹. Examples of these braided surfaces can be obtained by taking intersections of non-singular complex plane curves with 4-balls in \mathbb{C}^2 , and they can be used to study the links that arise as their boundaries in $S^3 = \partial D^4$ (see e.g. [42–44]).

Note that Rudolph's original definition of braided surface did not require the branched covering $S \rightarrow D^2$ to be simple. However, in the smooth category

¹Notice that we are reusing the function notation pr_2 , an abuse we will repeat in what follows. Indeed, we will be working with a number of spaces which admit some preferred product structure, and on each such space we let pr_2 denote projection to the second factor.

any non-simple braided surface can be taken via an arbitrarily small isotopy through braided surfaces to one whose branched covering $S \rightarrow D^2$ is simple. Thus we are free to assume that all of the critical points of our braided surfaces are indeed simple branch points. In a neighborhood of any such simple branch point $p \in S \subset D^2 \times D^2$, there are local complex coordinates (z, w) on $D^2 \times D^2$ such that S is given by the equation $z = w^2$. We say that p is a *positive* branch point if these coordinates can be taken to be orientation preserving, and a *negative* branch point otherwise.

The boundary of $D^2 \times D^2$ decomposes as $\partial(D^2 \times D^2) = (D^2 \times S^1) \cup (S^1 \times D^2)$ in the obvious way, and we set $\partial_1 = D^2 \times S^1$ and $\partial_2 = S^1 \times D^2$. We identify $\partial(D^2 \times D^2)$ with S^3 , by matching the product structure of ∂_1 with T_1 , and ∂_2 with T_2 . Under this identification we can consider closed braids in $\partial(D^2 \times D^2)$ as links in ∂_1 on which the projection $\text{pr}_2 : \partial_1 \rightarrow S^1$ restricts to a covering map. Notice then that the boundary of a braided surface is a closed braid in $\partial(D^2 \times D^2)$.

One feature of Rudolph's braided surfaces are that they are all necessarily *ribbon*. A properly embedded surface S in $D^4 = \{(z, w) : |z|^2 + |w|^2 \leq 1\}$ is said to be *ribbon embedded* if the function $|z|^2 + |w|^2$ restricts to S as a Morse function with no local maximal points. A properly embedded surface is said to be *ribbon* if it is isotopic to a surface which is ribbon embedded. By fixing an identification of $D^2 \times D^2$ with D^4 , we can similarly consider ribbon surfaces in $D^2 \times D^2$ (the definition of ribbon embeddings in $D^2 \times D^2$ will depend on our choice of identification, though the resulting class of ribbon surfaces will not).

Rudolph proved that any ribbon surface in $D^2 \times D^2$ is isotopic to a braided

surface. His algorithm proceeds first by pushing the surface S to the boundary of $D^2 \times D^2$, so that it sits as a ribbon immersed surface in S^3 . A band decomposition of S is then used as the surface is rearranged to the desired position. Note that even if ∂S is already a closed braid in $\partial(D^2 \times D^2)$, Rudolph's algorithm does not in general allow us to keep ∂S fixed during the isotopies.

Viro defined a similar notion which he called a *2-braid*, by requiring that $\partial S \subset \partial_1 = D^2 \times S^1$ be a trivial closed braid (i.e. $\partial S = P \times S^1$ for some finite subset $P \subset D^2$). 2-braids come equipped with a closure operation yielding closed surfaces in S^4 , and Viro [46] proved a 4-dimensional Alexander theorem by showing that every closed oriented surface in S^4 is isotopic to the closure of a 2-braid. These 2-braids were also studied extensively by Kamada [26–30], who proved a 4-dimensional Markov theorem relating any two 2-braids with isotopic closures.

2.3 Braided link cobordisms in $S^3 \times [0, 1]$

For much of what follows, it will be necessary to study a more general class of braided surfaces. Suppose $W \subset S^3 \times [0, 1]$ is an oriented surface, embedded smoothly and properly. Let $\text{pr}_2 : S^3 \times [0, 1] \rightarrow [0, 1]$ be the projection, and let $\text{pr}_W : W \rightarrow [0, 1]$ be its restriction to W . If t is a regular value of pr_W , then $W_t := \text{pr}_W^{-1}(t)$ will be a link in $S^3 \times \{t\}$, which for $t < 1$ we orient as the boundary of $W_{[t, 1]} := \text{pr}_W^{-1}([t, 1])$.

Now suppose that pr_W defines a Morse function on W , and that

1. W_t is a closed braid for each regular value t , and

2. W_t contains a single critical point for each critical value t .

Then we say that W is a *braided link cobordism* (or simply a *braided cobordism*). The regular level sets of a braided cobordism in $S^3 \times [0, 1]$ are all closed braids, and passing any critical value changes this braid by either a saddle point surgery, or the addition or deletion of a single component around the braid axis.

2.4 Braided cobordisms from braided surfaces

Braided cobordisms are closely related to braided surfaces, a fact which we illuminate here. We have already specified an identification of $\partial(D^2 \times D^2)$ with S^3 above. For $0 \leq t \leq 1$, we can scale $\partial(D^2 \times D^2)$ by a factor of $\frac{1}{2}(t+1)$ and identify it with $S^3 \times \{t\}$. In such a way we obtain an identification of $S^3 \times [0, 1]$ with a collar neighborhood of $\partial(D^2 \times D^2)$ in $D^2 \times D^2$.

As any properly embedded surface S in $D^2 \times D^2$ can easily be arranged to lie in a collar neighborhood of $\partial(D^2 \times D^2)$, we see that after smoothing corners any such surface gives rise to a smooth properly embedded surface in $S^3 \times [0, 1]$ whose boundary lies in $S^3 \times \{1\}$, and vice versa.

Suppose now that $S \subset D^2 \times D^2$ is a braided surface. Recall that $\text{pr}_2 : D^2 \times D^2 \rightarrow D^2$ restricts to a branched covering on S , and that it restricts to give projections $\partial_1 \rightarrow S^1$ and $\partial_2 \rightarrow D^2$. After an isotopy of S in $D^2 \times D^2$ which preserves the fibers of the projection pr_2 , we can assume that all of the branch points of S lie in $\partial_1 \times [0, 1]$ (in the usual collar neighborhood product structure). Then the $S \cap (\partial_2 \times [0, 1])$ will be a collection of disks, each of which is mapped homeomorphically onto its image by pr_2 . After another isotopy

we can also assume that each of these disks is of the form $\{p\} \times D^2 \times \{t\}$ in $\partial_2 \times [0, 1] = S^1 \times D^2 \times [0, 1]$.

Consider now the surface $W \subset S^3 \times [0, 1]$ associated to S by the above identification. Let $W_t = W \cap (S^3 \times \{t\})$ for some t . The projection $\text{pr}_2 : T_1 \rightarrow S^1$ then induces a (possibly singular) covering of $W_t \cap (T_1 \times \{t\})$ over S^1 . Likewise $\text{pr}_2 : T_2 \rightarrow D^2$ induces a covering of $W_t \cap (T_2 \times \{t\})$ over D^2 . Thus W_t will consist of a (possibly singular) closed braid in $T_1 \times \{t\}$, and a collection of disks in $T_2 \times \{t\}$. The singular points of the closed braid consist of pairs of transversely intersecting strands, and correspond to branch points of S . The disks each intersect the braid axis transversely in a single point, and each one realizes a local minimum of $W \subset S^3 \times [0, 1]$ with respect to the $[0, 1]$ coordinate.

Consider now how the sets W_t change as we let t range from 1 to 0. To start, W_1 will be a closed braid in $\partial_1 \times \{1\}$. As we let t decrease, we will see a continuous family of closed braids, except at a finite collection of t -values. As we pass a singular t -value corresponding to a branch point of S , we see a pair of strands merge together at the branch point, then separate again with a different crossing structure. As we approach a singular t -value t_0 corresponding to a disk, for $t > t_0$ we see a closed loop in $T_1 \times \{t\}$, which approaches the common boundary of $T_1 \times \{t\}$ and $T_2 \times \{t\}$ as $t \rightarrow t_0$. When $t = t_0$ this loop is capped off with the disk in $T_2 \times \{t_0\}$, and hence it does not appear at levels with $t < t_0$.

After a small isotopy supported in the neighborhood of this disk, we can arrange that instead of capping the loop off, as $t \rightarrow t_0$ it instead shrinks to a point on the braid axis, and then vanishes. The path traced by this loop as

it shrinks and vanishes gives a neighborhood in the new surface of an isolated local minimal point.

After these local modifications it is not hard to see then, that W is a braided cobordism, which is ribbon embedded and has $W \cap (S^3 \times \{0\}) = \emptyset$. Conversely, any braided cobordism with these properties gives rise to a braided surface in $D^2 \times D^2$. If the braided surfaces S and S' are isotopic via an isotopy passing entirely through braided surfaces, then the corresponding braided cobordisms W and W' will be isotopic via an isotopy passing entirely through braided cobordisms, and conversely.

2.5 Braided surfaces with caps

Now suppose that $W \subset S^3 \times [0, 1]$ is a braided cobordism, with $W \cap (S^3 \times \{0\}) = \emptyset$, which is *not* ribbon (i.e. has local maximal points in $S^3 \times (0, 1)$). Then the corresponding surface S in $D^2 \times D^2$ will not be ribbon, and hence will not be a braided surface. However, W can be isotoped to a *braided surface with caps*, which we define below.

Let $\phi : F \rightarrow \Sigma$ be a smooth map of oriented surfaces. Then a *cap of F with respect to ϕ* is an embedded disk $D \subset F$, so that

1. ϕ restricts to embeddings on $\text{int } D$ and on ∂D ,
2. F and Σ both admit coordinate charts of the form $S^1 \times [-1, 1]$ around $\partial D = S^1 \times \{0\}$ and $\phi(\partial D) = S^1 \times \{0\}$, on which ϕ is given by $(\theta, t) \mapsto (\theta, t^2)$,
3. in the above coordinate chart around $\phi(\partial D)$, the curve $S^1 \times \{1\}$ lies in

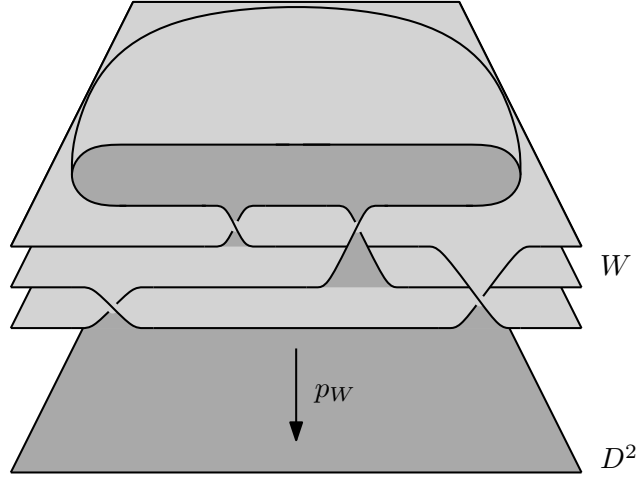


Figure 2.1: Braided surface with caps

$\phi(\text{int } D)$.

Now let $S \subset D^2 \times D^2$, and let pr_S denote the restriction of pr_2 to S . We say that S is a *braided surface with caps* if the critical points of pr_S all correspond either to isolated branch points or to boundaries of caps of S with respect to pr_S . Moreover, we require that the critical values in D^2 form a set of embedded concentric circles (corresponding to the boundaries of caps), with isolated critical values lying inside the innermost circle. See Figure 2.1 for a cross sectional diagram of a braided surface with a single cap.

Arguing as before, it is not hard to see that under the above identification of $S^3 \times [0, 1]$ with a collar neighborhood of $\partial(D^2 \times D^2)$, each braided cobordism disjoint from $S^3 \times \{0\}$ gives rise to a braided surface with caps in $D^2 \times D^2$, which is unique up to isotopies through braided surfaces. Each local maximal point in the braided cobordism gives rise to a cap in the braided surface.

Going the opposite direction, from a braided surface to a braided cobordism as in Section 2.4, is more difficult in the presence of caps however, as the

boundary of the cap might link non-trivially with other sheets of S . Such a surface S , when thought of as sitting in $S^3 \times [0, 1]$, can still be braided by Theorem 1.4.1, though the procedure will be more complicated than outlined above.

2.6 Summary of surface braidings

We summarize the previous discussion in the diagram below. All surfaces are assumed to be oriented, smoothly and properly embedded in their respective spaces.

$$\begin{array}{ccccc}
 \left\{ \begin{array}{c} \text{cobordisms} \\ \text{in } S^3 \times (0, 1] \end{array} \right\} & \supset & \left\{ \begin{array}{c} \text{braided cobordisms} \\ \text{in } S^3 \times (0, 1] \end{array} \right\} & \supset & \left\{ \begin{array}{c} \text{ribbon embedded} \\ \text{braided cobordisms} \\ \text{in } S^3 \times (0, 1] \end{array} \right\} \\
 \Updownarrow & & \Downarrow & & \Updownarrow \\
 \left\{ \begin{array}{c} \text{surfaces} \\ \text{in } D^2 \times D^2 \end{array} \right\} & \supset & \left\{ \begin{array}{c} \text{braided surfaces} \\ \text{with caps} \end{array} \right\} & \supset & \left\{ \text{braided surfaces} \right\}
 \end{array}$$

In what follows we will use cobordisms in $S^3 \times [0, 1]$ to prove the braiding results we need, but use braided surfaces with caps in $D^2 \times D^2$ for our applications. Hence we do not need to worry about passing from braided surfaces with caps to braided cobordisms.

Chapter 3

Braiding link cobordisms

This section is devoted to the proof of Theorem 1.4.1. After presenting a diagrammatic method for describing (braided) cobordisms, we begin the proof by collecting all critical points (with respect to the t -coordinate) of like index together, and braiding W around these critical points. This reduces the problem to braiding critical point free cobordisms, which we accomplish by applying a strengthened version of Morton's proof of the Markov theorem.

3.1 Movie presentations of braided cobordisms

For notational convenience during the proof of Theorem 1.4.1, we work with cobordisms in $\mathbb{R}^3 \times [0, 1]$ instead of $S^3 \times [0, 1]$. More precisely, pick a point $p \in U \subset S^3$ and identify the complement of p in (S^3, U) with $(\mathbb{R}^3, z\text{-axis})$. Choose the identification so that $\arg(w)$ corresponds with the angular cylindrical coordinate on \mathbb{R}^3 . Here we let (x, y, z) denote the usual coordinates on \mathbb{R}^3 , while t denotes the coordinate on $[0, 1]$.

We also must establish a diagrammatic method for describing braided cobordisms. Let $\pi : \mathbb{R}^3 \rightarrow \mathbb{R}^2$ denote the orthogonal projection to the xy -plane. After perturbing W slightly if necessary, we can assume that $\pi \times \text{id} : \mathbb{R}^3 \times [0, 1] \rightarrow \mathbb{R}^2 \times [0, 1]$ restricts to a family of regular link projections on W_t for all but finitely many $t \in (0, 1)$. After decorating with over and under crossing information, we obtain a continuous family of link diagrams with finitely many singular diagrams. Passing any such singular still changes the diagram by a Reidemeister move, adding or deleting a small circle, or the projection of a saddle point surgery. We refer to this family of link diagrams as the *movie presentation* of W . For each still which is a (nonsingular) link diagram, we equip it with the orientation induced by W_t , yielding the *oriented movie presentation* of W . Note that because we are not assuming W is in general position with respect to the z and t -projections, our definition of movie presentation differs slightly from that used by other authors (see e.g. [9]).

Now if W is a braided cobordism then the regular diagrams of its movie presentation will all be diagrams of closed braids, while passing a singular still will change the diagram by either:

1. addition or deletion of a single loop around $0 \in \mathbb{R}^2$ disjoint from the rest of the diagram,
2. addition or deletion of a single crossing between adjacent strands in the braid diagram by a band surgery,
3. a single braid-like Reidemeister move of type II or III, where each strand involved in the move is oriented in the positive direction.

We call such a movie presentation *braided*.

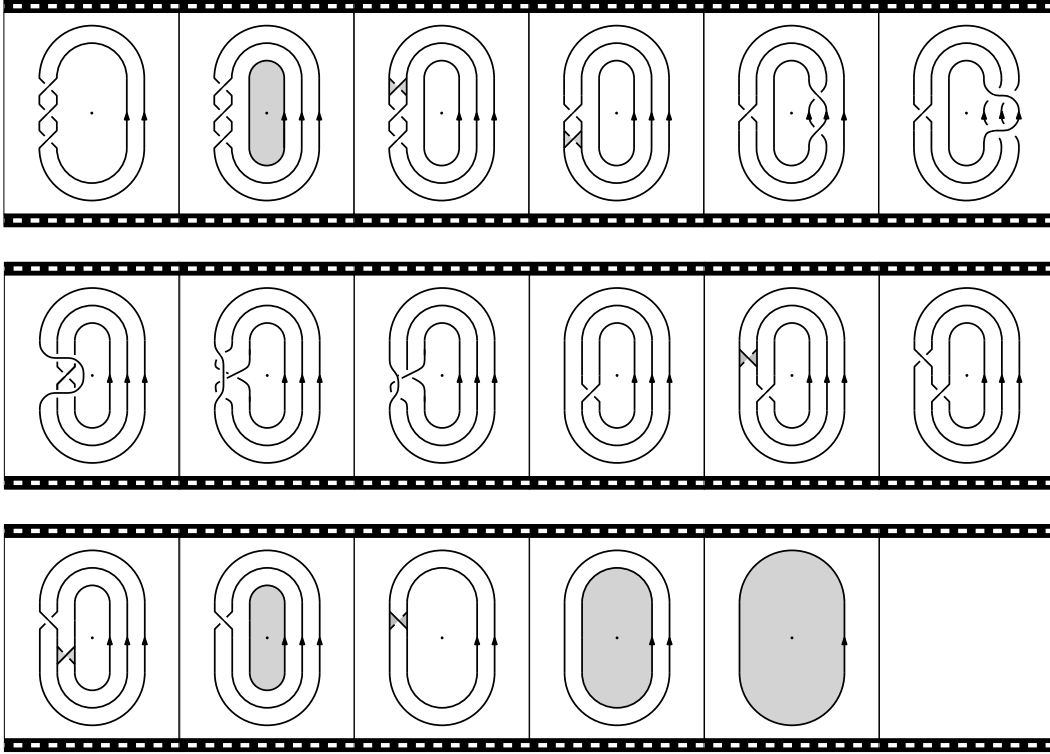


Figure 3.1: Braided movie presentation of a braided cobordism between the trefoil and the unknot

Thus if W is a braided cobordism its movie presentation is braided, and conversely. In this case W can be described by taking a finite number of the nonsingular stills, where each one differs from the previous still by a single modification as described above, or by a planar isotopy preserving the closed braid structure. We will often describe the movie presentation of a surface by such a sequence of diagrams. Some caution is needed in using such descriptions, as different choices of planar isotopies linking two adjacent diagrams can result in non-isotopic embeddings (see e.g., [24]). See Figure 3.1 for a genus 1 example of a braided movie presentation between the trefoil and the empty knot (the stills are read as lines of text, from left to right).

3.2 Braiding around critical points

We begin with the proof of Theorem 1.4.1. Suppose that $W \subset \mathbb{R}^3 \times [0, 1]$ is a properly embedded oriented link cobordism between closed braids $B_0 \subset \mathbb{R}^3 \times \{0\}$ and $B_1 \subset \mathbb{R}^3 \times \{1\}$. For any such surface $W \subset \mathbb{R}^3 \times [0, 1]$ and any $[a, b] \subset [0, 1]$, let $W_{[a,b]} = W \cap (\mathbb{R}^3 \times [a, b])$.

Lemma 3.2.1. *There is an isotopy of W rel ∂W , taking W to a surface W' such that $W'_{[a,b]}$ is a braided cobordism for $[a, b] \in \{[0, \frac{1}{6}], [\frac{1}{3}, \frac{2}{3}], [\frac{5}{6}, 1]\}$, and is free of critical points for $[a, b] \in \{[\frac{1}{6}, \frac{1}{3}], [\frac{2}{3}, \frac{5}{6}]\}$.*

Proof. As both B_0 and B_1 are closed braids, W_t will also be a closed braid for t close to 0 and 1, and so we can assume that W_t is a closed braid for all $t \in [0, \frac{1}{6}] \cup [\frac{5}{6}, 1]$. Push all minimal points into $\mathbb{R}^3 \times [0, \frac{1}{6}]$, all maximal disks into $\mathbb{R}^3 \times [\frac{5}{6}, 1]$, and all saddle points into $\mathbb{R}^3 \times \{\frac{1}{2}\}$ (see [30] for details). The maximal and minimal points can clearly be positioned in such a way that $W'_{[0, \frac{1}{6}]}$ and $W'_{[\frac{5}{6}, 1]}$ remain braided.

Now passing each saddle point changes the level set W_t by surgery along a 2-dimensional 1-handle. After a small perturbation in a neighborhood of each saddle point, we can assume that these 1-handles all lie in $\mathbb{R}^3 \times \{\frac{1}{2}\}$. By adding a half-twist in each band, we can arrange that each segment of $W_{\frac{1}{2}+\varepsilon}$ and $W_{\frac{1}{2}-\varepsilon}$ involved in the surgeries are oriented in the positive direction (see Figure 3.2, where $W_{\frac{1}{2}}$ is shown). Keeping these bands in place, the remaining strands of $W_{\frac{1}{2}}$ can be braided using the standard proof of the classical Alexander's theorem. Thus we can arrange $W_{\frac{1}{2}}$ so that it is a closed braid both before and after the surgeries, and can extend the closed braid structure to the rest of $W'_{[\frac{1}{3}, \frac{2}{3}]}$. □

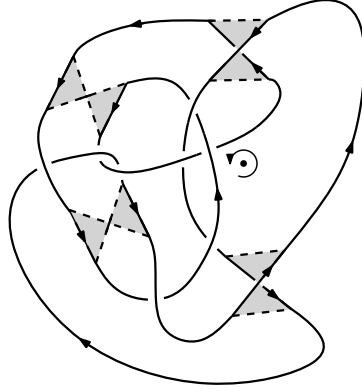


Figure 3.2: Braiding saddle points

The above argument is due to Kamada [30]. To prove Theorem 1.4.1, it thus suffices to prove it for critical point free cobordisms between closed braids.

3.3 Braiding critical point free cobordims

Any cobordism W which is free of critical points is topologically just a union of cylinders, and is isotopic to a product cobordism. In general, however, the isotopy taking W to a product cobordism cannot be chosen to fix the boundary. Consider, for example, the movie presentation of the cobordism W depicted in Figure 3.3. The middle still is meant to imply that the bottom strand is given a non-zero number of full twists as we look at the level sets moving down. The top and the bottom stills are the same closed braid L , and hence W is isotopic to $L \times [0, 1]$. It is not hard to verify that there are no boundary fixing isotopies joining these two cobordisms, however. Indeed, we can think of W and $L \times [0, 1]$ as sitting in S^4 via the natural inclusion $S^3 \times [0, 1] \hookrightarrow S^4$. Then W and $L \times [0, 1]$ can be capped off in such a way that they yield a twist-spun trefoil and spun trefoil respectively. These 2-knots are not isotopic in S^4 , as

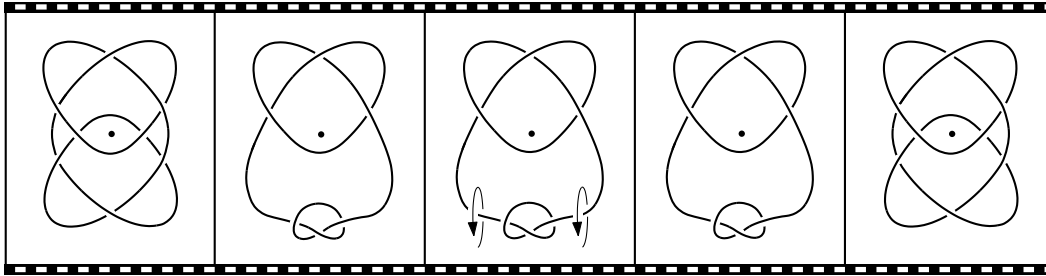


Figure 3.3: Critical point free cobordism not isotopic rel boundary to product cobordism

can be seen by computing the fundamental groups of their complements (see [9, 47], for example). In fact, if the bottom strand is given precisely one twist, then the resulting twist-spun trefoil is just an unknotted sphere in S^4 .

The movie presentations of a critical point free cobordism is described entirely via sequences of Reidemeister moves and planar isotopies. We will complete the proof of Theorem 1.4.1 in two stages, first by proving it for critical point free cobordisms whose movie presentation is described entirely by a planar isotopy (i.e. no Reidemeister moves take place between nearby stills) before proving it for the general case. Before doing this however, we must first recall a geometric set of Markov moves for classical links used by Morton in [39], as well as his diagram threading construction which gives a diagrammatic approach to studying isotopies of closed braids.

3.4 Geometric Markov moves for closed braids in \mathbb{R}^3

Morton's geometric formulation of Markov's theorem states that two closed braids which are isotopic as links can be joined by a sequence of braid isotopies

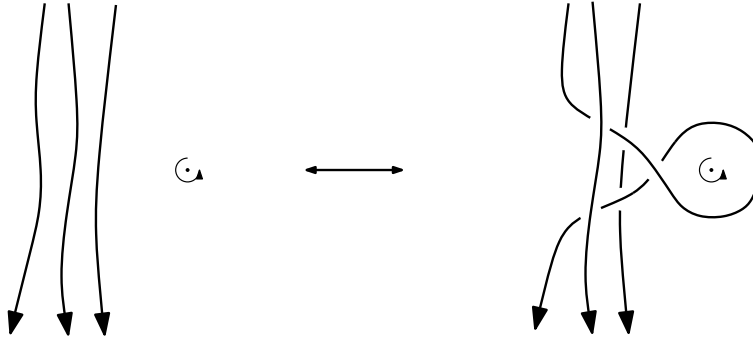


Figure 3.4: Simple Markov equivalence

and simple Markov equivalences. A *braid isotopy* between two closed braids L_0 and L_1 in \mathbb{R}^3 is an isotopy ϕ_α of \mathbb{R}^3 (i.e. a continuous family of maps $\phi_\alpha : \mathbb{R}^3 \rightarrow \mathbb{R}^3$ parametrized by $\alpha \in [0, 1]$, with $\phi_0 = \text{id}_{\mathbb{R}^3}$), such that $\phi_\alpha(L_0)$ is a closed braid for all α , and $\phi_1(L_0) = L_1$.

The second move on closed braids is a geometric version of braid stabilization. Let B and B' be closed braids, and suppose there is an oriented embedded disk $D \subset \mathbb{R}^3$ intersecting the z -axis transversely in a single point. Suppose also that $\partial D = c \cup c'$, where $c = B \cap D$ and $c' = B' \cap D$ are connected and where the boundary orientation of ∂D is winding clockwise along c , and counterclockwise along c' . Suppose further that $B \setminus c = B' \setminus c'$. Then B and B' are said to be *simply Markov equivalent* (see Figure 3.4).

The projections of such B and B' to the xy -plane differ by a sequence of Reidemeister moves which includes precisely one move of type I, creating an extra loop around the origin (see Figure 3.4).

3.5 Threading construction

We now recall Morton's diagram threading technique and use it to show that any link isotopy can be deformed into one that passes through closed braids everywhere except at a finite number of critical points we must necessarily introduce. All this will be done while keeping the starting and ending links fixed.

Let $P = \{xz\text{-plane}\}$ and let $\rho : \mathbb{R}^3 \rightarrow P$ be the orthogonal projection. Let $h \subset P$ be the image of the z -axis (braid axis) under ρ . Suppose D is the diagram in P of an oriented link L . Let $C \subset D$ denote the double points (crossings) of L under the projection ρ .

A *choice of overpasses* for D is a pair of disjoint finite subsets $S, F \subset D \setminus C$, so that each link component contains a points from $S \cup F$, and so that points of S alternate with points of F when traveling along any component. Furthermore when traveling in the positively oriented direction, each arc of the form $[s, f]$ contains no undercrossings, and each arc $[f, s]$ contain no overcrossings.

Now let $P_+ = \{x > 0 \text{ (right) half-plane of } P\}$ and $P_- = \{x < 0 \text{ (left) half-plane of } P\}$ be the two regions of P separated by h . Although h is not a component of the link L , we can enhance the diagram D by assigning crossing choices whenever D intersects h transversely.

Given such an enhanced diagram, h is said to *thread* the diagram D for some choice of overpasses (S, F) , if h intersects D in transverse double points, $S \subset P_-$, $F \subset P_+$, and

1. when traveling from P_- to P_+ , D crosses over h ,
2. when traveling from P_+ to P_- , D crosses under h .

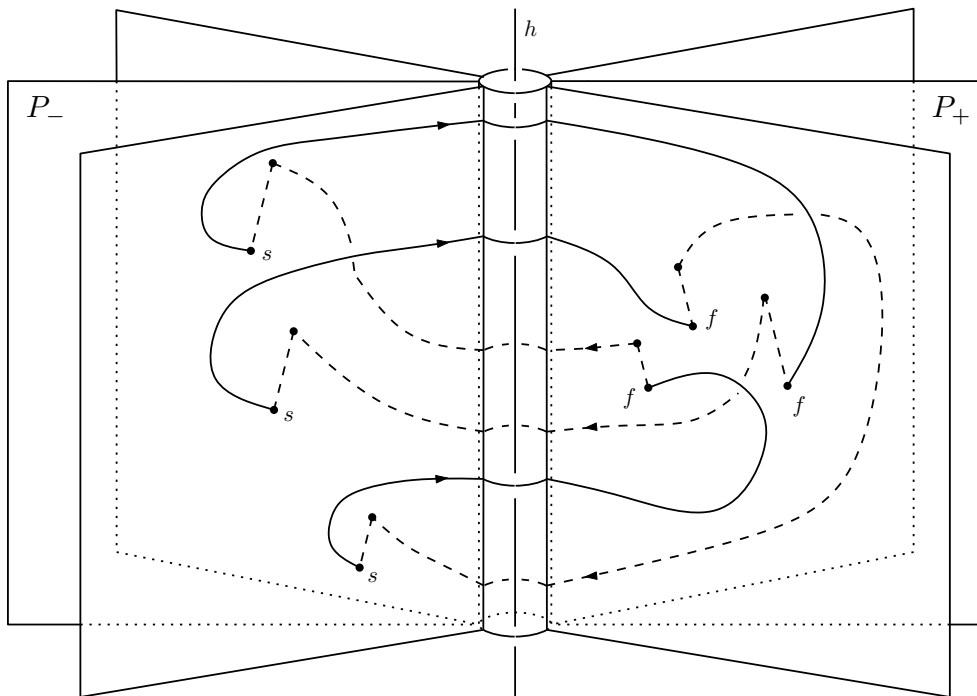


Figure 3.5: Trefoil as a closed braid given by a threading

Threadings of link diagrams allow us to study closed braids on the level of link diagrams. The following lemma is due to Morton (see [39]):

Lemma 3.5.1. *Suppose D is a diagram that is threaded by h for some choice of overpasses. Then there is a closed braid L with diagram D .*

The idea behind the proof of the lemma is summarized in Figure 3.5. Conversely, it is also easy to show that any closed braid is braid isotopic to one whose diagram is threaded by h for some choice of overpasses.

3.6 Braiding movie presentations without Reidemeister moves

Now suppose that $W \subset \mathbb{R}^3 \times [0, 1]$ is a critical point free cobordism between two closed braids, and consider the movie presentation of W , this time projecting each $W_t \subset \mathbb{R}^3 \times \{t\} = \mathbb{R}^3$ to the plane P via the projection ρ . We let D_t denote the (possibly singular) diagram of W_t in P for each $t \in [0, 1]$. As W is free of critical points, nearby diagrams will differ by either a planar isotopy or Reidemeister move. If the movie presentation of W does not involve any Reidemeister moves, then it can be described completely by specifying the initial diagram D_0 and a planar isotopy ϕ_α of P , with $\phi_t(D_0) = D_t$ for all t . In what follows it will be convenient to specify the movie presentations of such surfaces in this way.

We prove Theorem 1.4.1 first in the special case when D_0 and D_1 are threaded, and the movie presentation of W does not involve any Reidemeister moves:

Proposition 3.6.1. *Suppose W has no critical points, and that its movie presentation does not involve any Reidemeister moves. Suppose further that W_0 and W_1 are closed braids with diagrams D_0 and D_1 threaded by h for some choices of overpasses. Then W is isotopic relative its boundary to a braided cobordism.*

In order to prove the above proposition we will need to lift the planar isotopy joining D_0 and D_1 to a sequence of braid isotopies and simple Markov equivalences in \mathbb{R}^3 . For the rest of this section we assume W is as described

in the statement of Proposition 3.6.1. The first lemma we will need is the following:

Lemma 3.6.2. *Let ψ_α be a planar isotopy of P taking D_0 to D_1 which fixes h setwise. Suppose further that $\psi_\alpha \equiv \psi_0$, and $\psi_{1-\alpha} \equiv \psi_1$ for α in small neighborhoods of 0 and 1 respectively. Then there is a braid isotopy ϕ_α taking W_0 to W_1 , such that $\rho \circ \phi_\alpha(W_0) = \psi_\alpha(D_0)$ for all $\alpha \in [0, 1]$.*

Proof. For any $p \in W_0$ and $\alpha \in [0, 1]$, the x and z -coordinate of $\phi_\alpha(p)$ are determined by ψ_α . The y -coordinate of $\phi_\alpha(p)$ can then be chosen uniquely so that the radial coordinate of $\phi_\alpha(p)$ remains constant for all α . It thus suffices to note that any two closed braids with the same diagram are also braid isotopic, via a straight line isotopy. \square

Let $(S_0, F_0), (S_1, F_1) \subset P$ denote the overpasses chosen for the threadings of D_0 and D_1 respectively, and let ψ_α denote a planar isotopy of P associated to the movie presentation of W , i.e. $\psi_\alpha(D_0) = D_\alpha$ for all $\alpha \in [0, 1]$. We can assume that

$$S_0 \cap \psi_1^{-1}(S_1) = F_0 \cap \psi_1^{-1}(F_1) = \emptyset.$$

The following lemma will allow us to assume that the choices of overpasses for both D_0 and D_1 coincide, and that they can be assumed to be fixed by the planar isotopy ψ_α .

Lemma 3.6.3. *W is isotopic relative its boundary to a cobordism whose movie presentation is determined by a planar isotopy φ_α , where $\varphi_\alpha(S_0) = S_0$ and $\varphi_\alpha(F_0) = F_0$ for $0 \leq \alpha \leq 1/2$, and where $\varphi_\alpha(\varphi_{1/2}^{-1}(S_1)) = S_1$ and $\varphi_\alpha(\varphi_{1/2}^{-1}(F_1)) = F_1$ for $1/2 \leq \alpha \leq 1$.*

Proof. We can assume that for all $q \in S_1 \cup F_1$, the sets $\{\psi_\alpha^{-1}(q) \mid 0 \leq \alpha \leq 1\}$ are disjoint embedded arcs in P which do not intersect $S_0 \cup F_0$ (see for example Lemma 10.4 of [8]). For each $q \in S_1 \cup F_1$ choose a small regular neighborhood A_q of $\{\psi_\alpha^{-1}(q) \mid 0 \leq \alpha \leq 1\}$, so that the A_q are pairwise disjoint and also do not intersect $S_0 \cup F_0$.

Now let ξ_α be a planar isotopy of P which restricts to the identity on the complement of $\bigcup A_q$, and such that for all $\alpha \in [0, 1]$ and all $p \in \psi_1^{-1}(S_1 \cup F_1)$ we have $\xi_\alpha(p) = \psi_{1-\alpha}^{-1} \circ \psi_1(p)$. Let $\Xi_{\tau, \alpha}$ be the one parameter family of planar isotopies of P defined by

$$\Xi_{\tau, \alpha} = \begin{cases} \xi_{2\tau\alpha} & \text{if } 0 \leq \alpha \leq 1/2 \\ \xi_{\tau(2-2\alpha)} & \text{if } 1/2 \leq \alpha \leq 1. \end{cases}$$

After an isotopy of W which rescales the t -coordinate, we can arrange so that the movie presentation of W is instead described by the planar isotopy

$$\Phi_\alpha = \begin{cases} \text{id} & \text{if } 0 \leq \alpha \leq 1/2 \\ \psi_{2\alpha-1} & \text{if } 1/2 \leq \alpha \leq 1. \end{cases}$$

Now consider the composition $\Phi_\alpha \circ \Xi_{\tau, \alpha}$. Letting τ range from 0 to 1 shows that the surface W , which is described by the diagram D_0 and the planar isotopy $\Phi_\alpha = \Phi_\alpha \circ \Xi_{0, \alpha}$, is isotopic to a surface described by D_0 and the planar isotopy

$$\varphi_\alpha := \Phi_\alpha \circ \Xi_{1, \alpha} = \begin{cases} \xi_{2\alpha} & \text{if } 0 \leq \alpha \leq 1/2 \\ \psi_{2\alpha-1} \circ \xi_{2-2\alpha} & \text{if } 1/2 \leq \alpha \leq 1. \end{cases}$$

As the ξ_α is the identity outside of $\bigcup A_q$, for any $p \in S_0 \cup F_0$ and any $\alpha \in [0, 1/2]$ we have $\varphi_\alpha(p) = \xi_{2\alpha}(p) = p$. Moreover, for $\alpha \in [1/2, 1]$ and $q \in \varphi_{\frac{1}{2}}^{-1}(S_1 \cup F_1) = \psi_1^{-1}(S_1 \cup F_1)$, we have

$$\varphi_\alpha(q) = \psi_{2\alpha-1} \circ \xi_{2-2\alpha}(q) = \psi_{2\alpha-1} \circ \psi_{1-(2-2\alpha)}^{-1} \circ \psi_1(q) = \psi_1(q) = \varphi_{\frac{1}{2}}(q)$$

as required. Note that all the isotopies described above fix $W_0 \cup W_1 = \partial W$. \square

By the above lemma it is enough to prove Proposition 3.6.1 in the case when $S = S_0 = S_1$, $F = F_0 = F_1$, and all points in $S \cup F$ are fixed by ψ_α . Indeed, since the points in $S_0 \cup F_0$ are stationary during the first half of the planar isotopy φ_α , and since they form a choice of overpasses for which D_0 is threaded, they must also form a choice of overpasses which give a threading of $D_{1/2}$. Likewise, $D_{1/2}$ is also threaded by h with the choice of overpasses (S_1, F_1) , since they remain stationary for during the second half of φ_α and give a threading of D_1 . By Lemma 3.5.1 we can arrange W locally near $\mathbb{R}^3 \times \{\frac{1}{2}\}$ so that $W_{1/2}$ is a closed braid with diagram $D_{1/2}$ threaded with either choice of overpasses.

Suppose then that W is as above. Although the movie presentation of W does not involve any Reidemeister moves, it will (after perturbing W slightly away from the boundary) contain Reidemeister-like moves of type II and III involving components of the diagrams and the z -axis h (see Figure 3.6). These Reidemeister-like moves are like classical Reidemeister moves, but where no crossing information is specified at double points of the projection involving h . The absence of crossing information with h reflects the fact that the movie presentation of W does not specify the relative position of the links W_t above

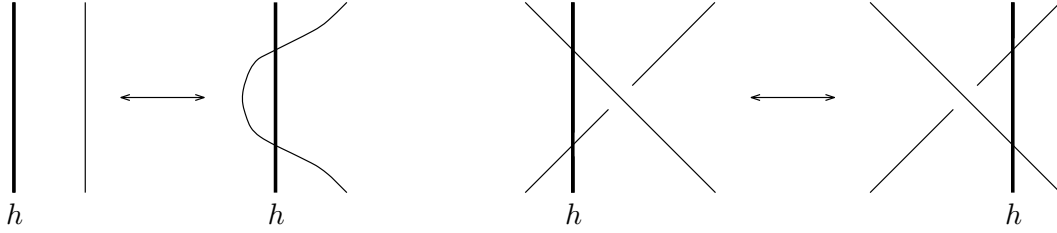


Figure 3.6: Reidemeister-like moves involving h

or below the plane P , and that the components of the link are free to pass through the z -axis during isotopies in \mathbb{R}^3 .

We can thus break the planar isotopy ψ_α determining W into a sequence of transformations that take into account the relative position of the diagrams D_t with h . More precisely, we can divide the interval $[0, 1]$ into smaller subintervals $[t_{j-1}, t_j]$, such that for each j there is either

1. a planar isotopy ϕ_α^j of P , which fixes h setwise and has $\phi_\alpha^j(D_{t_{j-1}}) = D_{t_{j-1} + \alpha(t_j - t_{j-1})}$ for all $\alpha \in [0, 1]$, or
2. a Reidemeister-like move of type II or III taking $D_{t_{j-1}}$ to D_{t_j} involving (but fixing) h .

We will simplify notation and write D^j and W^j instead of D_{t_j} and W_{t_j} respectively, for each j . Since we are assuming that the points of $S \cup F$ are fixed throughout the planar isotopy ψ_α , we can fix (S, F) as a choice of overpass for each D^j . Furthermore for each diagram we fix the unique choice of h -crossing information so that D^j is threaded by h .

Before proceeding, we need to eliminate any situations as in Figure 3.7. Here we have a Reidemeister-like move of type III where the center crossing cannot pass to the other side of h without first introducing crossing changes.

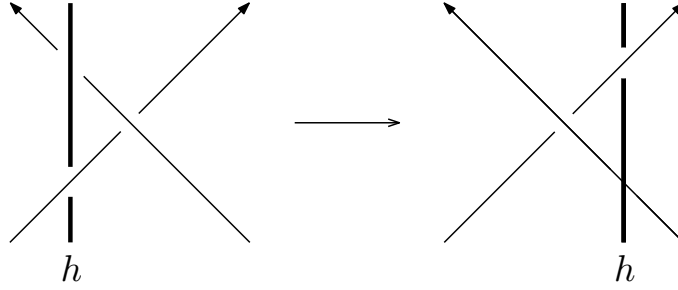


Figure 3.7: Reidemeister-like move of type III which does not lift to a braid isotopy

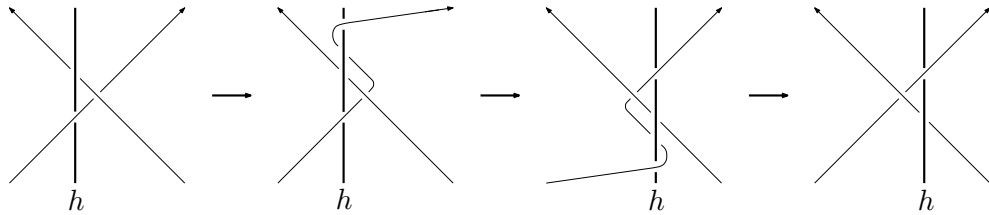


Figure 3.8: Replacing bad Reidemeister-like moves of type III with sequence of moves that lift to braid isotopies and simple Markov equivalences

These can be eliminated by making a local replacement as in Figure 3.8, where the offending move has been replaced by a sequence consisting of three Reidemeister-like moves, two of type II and one of type III (which lifts to an isotopy avoiding the z -axis). This local replacement does not change the isotopy class of W rel ∂W .

Lemma 3.6.4. *Suppose that W^{j-1} is a closed braid. Then the transformation $D^{j-1} \rightarrow D^j$ lifts to \mathbb{R}^3 as a sequence of braid isotopies and simple Markov equivalences on W^{j-1} .*

Proof. Note first that since W^{j-1} is a closed braid and D^{j-1} is threaded, the h -crossing information on D^{j-1} will match that coming from the projection of W^{j-1} .

For transformations of type (1) above, Lemma 3.6.2 shows that the planar

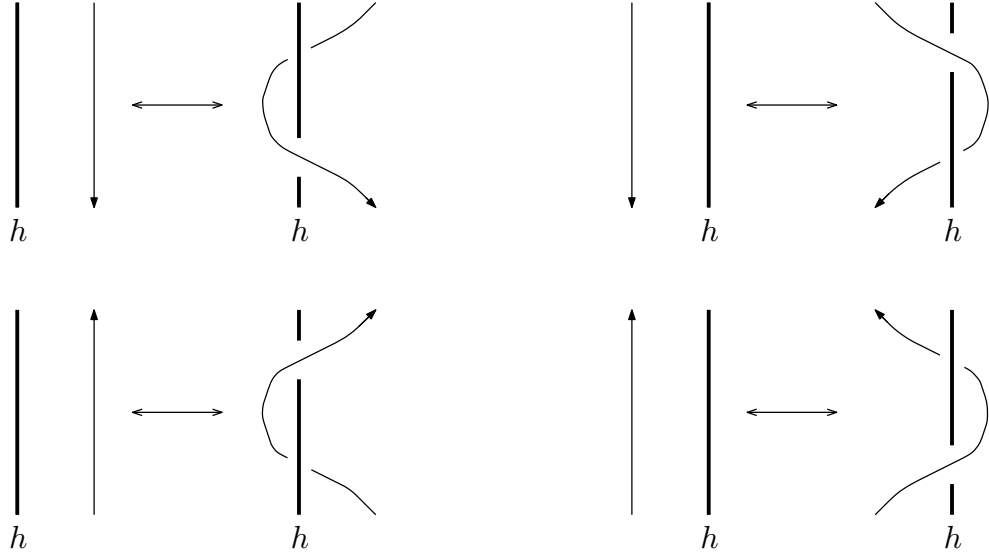


Figure 3.9: Reidemeister-like moves of type II

isotopy between D^{j-1} and D^j can be lifted to a braid isotopy on W^{j-1} .

Suppose now that D^j is obtained from D^{j-1} by a Reidemeister-like move of type II (or its inverse) as in Figure 3.6. Then as D^{j-1} is threaded, locally it must look like either the right or left-hand side of one of the transformations in Figure 3.9. Note that by assumption no points of S or F can occur anywhere in these local pictures. Clearly D^j can be lifted to a closed braid W^j which agrees with W^{j-1} away from the Reidemeister-like move of type II, so that W^{j-1} and W^j are simply Markov equivalent.

Now suppose that D^j is obtained from D^{j-1} by a Reidemeister-like move of type III. It is easy to verify that for most configurations of D^{j-1} the move can be lifted to a braid isotopy taking W^{j-1} to a closed braid W^j with diagram D^j . The only exceptions arise as in the Figure 3.7, but these were all replaced previously by sequences of moves that can be lifted. \square

Starting with the closed braid $W_0 \subset \mathbb{R}^3 \times \{0\}$, we can construct a new

surface W' by tracing the path of W_0 in $\mathbb{R}^3 \times [0, 1]$ as we apply the sequence of lifted braid isotopies and simple Markov equivalences obtained from the previous lemma. Away from the simple Markov equivalences each level set W'_t will be a closed braid. By construction, the movie presentation of W' will be the same as that of W , hence it will be isotopic to W rel $\partial W'$. To prove Proposition 3.6.1 it thus remains only to show that W can be braided in neighborhoods of the simple Markov equivalences.

Proof of Proposition 3.6.1. Suppose that for some $s \in [0, 1]$ and $\varepsilon > 0$ the closed braids $W_{s-\varepsilon}$ and $W_{s+\varepsilon}$ differ by a simple Markov equivalence joined by a disk D . After a small isotopy in the neighborhood of the hyperplane $\mathbb{R}^3 \times \{s\}$ we can assume that D lies entirely in this hyperplane, and that the orthogonal projection of ∂D to the xy -plane yields a figure eight.

Decompose D as the boundary sum of two closed disks D' and D'' (equipped with the orientation of W), where D' intersects the z -axis transversely in a single point and where $\partial D'$ is a simple curve which is strictly monotone in the angular direction (see Figure 3.10). Push D' to either $\mathbb{R}^3 \times \{s + \varepsilon\}$ or $\mathbb{R}^3 \times \{s - \varepsilon\}$ (depending on whether $\partial D'$ is monotone increasing or decreasing respectively) while keeping D'' fixed. This gives rise to a new maximal disk (resp. minimal disk) while D'' yields a new saddle band. After a slight local perturbation these new critical disks can be changed to isolated critical points, completing the proof of Proposition 3.6.1. □

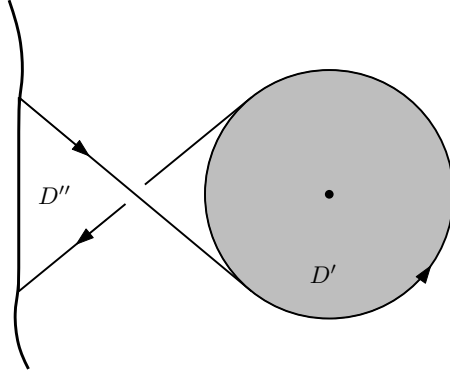


Figure 3.10: Decomposing a simple Markov equivalence into a pair of critical points

3.7 Braiding movie presentations with Reidemeister moves

Now consider an arbitrary critical point free cobordism W between two closed braids. The movie presentation of W under the projection to P will in general include Reidemeister moves as well as planar isotopies. Recycling notation from above, let D_t denote the diagram of W_t , and divide the interval $[0, 1]$ into smaller subintervals $[t_{j-1}, t_j]$, such that for each j there is either

1. a planar isotopy ϕ_α^j of P which has $\phi_\alpha^j(D_{t_{j-1}}) = D_{t_{j-1} + \alpha(t_j - t_{j-1})}$ for all $\alpha \in [0, 1]$, or
2. a Reidemeister move taking $D_{t_{j-1}}$ to D_{t_j} .

As above we will simplify notation and write D^j and W^j instead of D_{t_j} and W_{t_j} respectively, for each j . To complete the proof of Theorem 1.4.1 we need the following lemma:

Lemma 3.7.1. *Suppose D^j is obtained from D^{j-1} by a Reidemeister move of any type. Then there is a planar isotopy ζ_α of P , such that $\zeta_1(D^{j-1})$ and $\zeta_1(D^j)$ are both threaded by h for some choices of overpasses, and if W^{j-1} is a closed braid with diagram $\zeta_1(D^{j-1})$, then the Reidemeister move taking $\zeta_1(D^{j-1})$ to $\zeta_1(D^j)$ lifts to a braid isotopy of W^{j-1} .*

To see that this completes the proof of Theorem 1.4.1, note first that by Theorem 2 of [39] there are braid isotopies taking W_0 and W_1 to closed braids whose diagrams in P are threaded by h for some choices of overpasses. Thus we can assume that the diagrams D_0 and D_1 are both threaded. We also assume that in the movie presentation of W the sequence involved alternates between planar isotopies and Reidemeister moves, beginning and finishing with planar isotopies. Suppose for some j that D^j is obtained from D^{j-1} by a Reidemeister move, and let ϕ_α^{j-1} and ϕ_α^{j+1} be the planar isotopies taking D^{j-2} to D^{j-1} and D^j to D^{j+1} respectively. Then we can replace D^{j-1} and D^j with $\zeta_1(D^{j-1})$ and $\zeta_1(D^j)$ respectively, and ϕ_α^{j-1} and ϕ_α^{j+1} with $\zeta_\alpha \circ \phi_\alpha^{j-1}$ and $\zeta_{1-\alpha} \circ \phi_\alpha^{j+1}$ respectively, without changing the isotopy class of W rel ∂W . Performing a similar replacement one by one around all Reidemeister moves in the movie presentation, we see that W is isotopic relative its boundary to a cobordism whose movie presentation involves only Reidemeister moves and planar isotopies between threaded diagrams.

Thus we can assume that each of the D^j are threaded and that the W^j are all closed braids. By Proposition 3.6.1 the portions of W corresponding to planar isotopies in the movie presentation are then isotopic relative their boundaries to braided cobordisms, while by Lemma 3.7.1 we see that the same

is true for portions of W corresponding to Reidemeister moves. Thus W itself is isotopic relative its boundary to a braided cobordism, completing the proof.

Proof of Lemma 3.7.1. Begin by making a choice of overpasses for D^{j-1} and D^j which agree outside some small neighborhood of the move in question. In the small neighborhood of the move we choose points which give a valid choice of overpasses both before and after the move. See examples of different possible configurations in Figure 3.11, where incoming strands are labeled with o if they are part of an overpass, or u if they are part of an underpass.

Now let ζ_α be a planar isotopy which repositions all of the S points to the left ($x < 0$) half of the plane P , and all the F points on the right ($x > 0$) half of P . Once positioned in this way, there is a unique way to assign over and undercrossings of D^{j-1} and D^j with h so that both diagrams are threaded by h .

Note that in the case of moves of type I and II, we can choose S, F , and ζ_α so that the Reidemeister move of interest happens away from h . It is then easy to see that the Reidemeister move of interest lifts to a braid isotopy.

Moves of type III cannot be arranged to take place away from h however. Of the three strands in this local picture, one strand will cross over the other two, one will pass under the other two, while the third will pass over one and under the other. Choose S and F away from this picture so that the top strand is part of an overcrossing, the bottom strand is part of an undercrossing, and place a single point from each of S and F on the third strand to create a valid choice of overpasses.

Now we can arrange the diagrams so that h separates S and F , and so

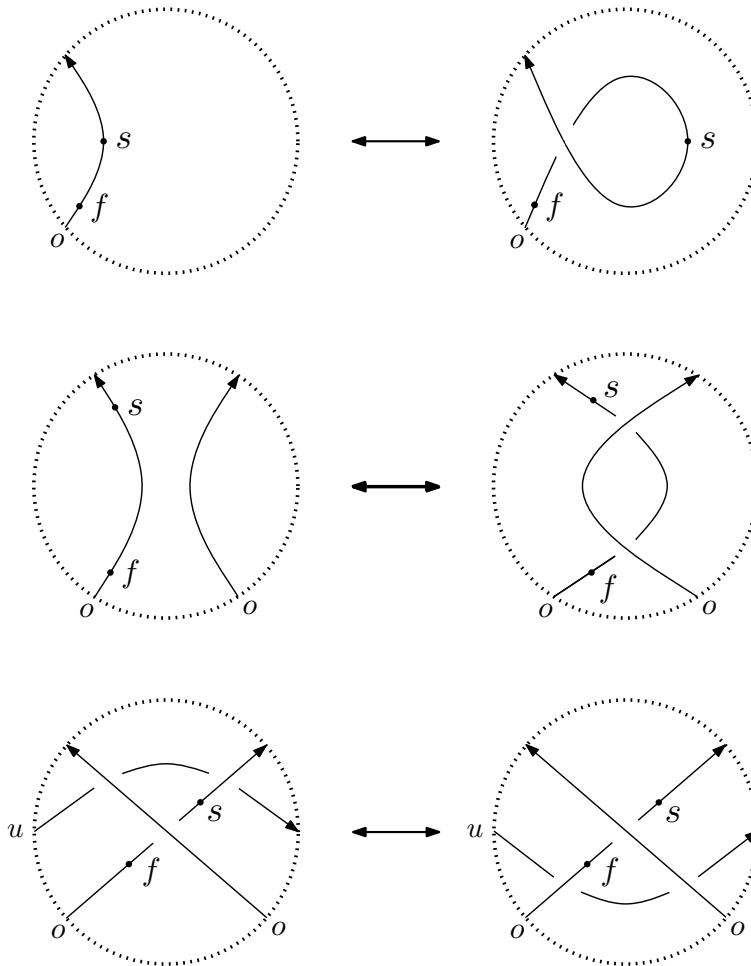


Figure 3.11: Overpass choices in a neighborhood of type I and II moves

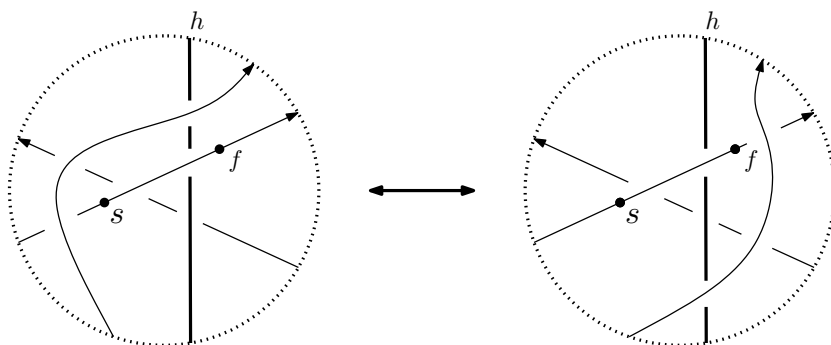


Figure 3.12: Threading near a Reidemeister move of type III

that the uppermost strand crosses over h in a neighborhood of the move (the orientation of this strand determines whether it will cross h at the top or bottom of the local picture). Regardless then of the orientation on the other two strands or their shared crossing, the uppermost strand is free to pass over the crossing and both the nearby S and F points as in Figure 3.12, a move which can clearly be lifted to a braid isotopy in \mathbb{R}^3 . This completes the proof of Lemma 3.7.1 and of Theorem 1.4.1. \square

Remark Suppose now that the cobordism W we start with is ribbon embedded (i.e. has no local maximal points with respect to the t -coordinate). Although we may hope to preserve this property during the braiding procedure described above, this will not be possible in general. Indeed, Morton [38] gave an example of a 4-strand braid β with closure the unknot which is *irreducible* (i.e. any sequence of Markov moves used to simplify β necessarily begins with a stabilization, raising the braid index to 5). As noted by Rudolph [42], it is not difficult to see that any braided ribbon surface bounded by the closure of β must then have genus ≥ 1 , even though it clearly bounds a ribbon disk in $S^3 \times [0, 1]$.

Chapter 4

Singular fibrations on smooth 4-manifolds

This chapter contains descriptions of the fibration structures we will be concerned with on 3 and 4-manifolds. Indeed, we present the definition of an *open book decomposition* on a closed 3-manifold, as well as the definition of a *broken Lefschetz fibration* (and its variants) on a smooth 4-manifold. We outline connections between these objects and (near-)symplectic structures on 4-manifolds, explain features of their topology in terms of handle decompositions, and describe some examples and constructions which will be needed for our proof of Theorem 1.4.4.

4.1 Open book decompositions of 3-manifolds

Let M be a closed oriented smooth 3-manifold. An *open book decomposition* on M is a smooth map $\lambda : M \rightarrow D^2$ such that $\lambda^{-1}(\partial D^2)$ is a compact 3-

dimensional submanifold on which λ restricts as a surface bundle over $S^1 = \partial D^2$. Furthermore, we require that the closure of $\lambda^{-1}(\text{int } D^2)$ is the disjoint union of solid tori $D^2 \times S^1$, on which λ is the projection $D^2 \times S^1 \rightarrow D^2$. We say that $\lambda^{-1}(0)$ is the *binding* of the open book on M , and that for any $p \in S^1$ the compact surface $\Sigma_p = \lambda^{-1}(\{\alpha \cdot p \mid 0 \leq \alpha \leq 1\})$ is the *page* over p .

By a celebrated theorem of Giroux, open book decompositions on a closed 3-manifold M (up to a positive stabilization operation) are in one-to-one correspondence with contact structures on M (up to isotopy). Thus open book decompositions provide a useful topological setting in which to study contact structures on a given closed 3-manifold.

4.2 Singular fibrations on 4-manifolds

Now let X be a smooth 4-manifold and Σ a compact surface, and let $f : X \rightarrow \Sigma$ be a smooth map. A critical point of f is called a *Lefschetz critical point* if there are orientation preserving local complex coordinates on which $f : \mathbb{C}^2 \rightarrow \mathbb{C}$ is modeled as $f(u, v) = u^2 + v^2$. If these coordinates around the critical point are instead orientation reversing, then it is called an *anti-Lefschetz critical point*.

An embedded circle $C \subset X$ of critical points of f is called a *round 1-handle singularity* or *broken singularity* if f is modeled near points of C by the map $(\theta, x, y, z) \mapsto (\theta, x^2 + y^2 - z^2)$ from $\mathbb{R} \times \mathbb{R}^3 \rightarrow \mathbb{R} \times \mathbb{R}$, where C is given locally by $x = y = z = 0$.

A surjective map $f : X \rightarrow \Sigma$ is called a *Lefschetz fibration* if all critical points of f are in the interior of X and are Lefschetz critical points. It is called an *achiral Lefschetz fibration* if we also allow anti-Lefschetz critical points.

Finally, we add the adjective *broken* to either of these names to indicate that we also allow round 1-handle singularities in the set of critical points of f . When discussing these maps we will sometimes use the generic term *fibration* to describe a map which can be any of the types defined above.

4.3 Boundary conditions on fibrations

Now suppose that $\partial X \neq \emptyset$ is connected, and that $f : X \rightarrow \Sigma$ is a Lefschetz fibration (possibly broken, possibly achiral). Then we say that f is *convex*, if

- $\Sigma = D^2$,
- $f(\partial X) = D^2$, and
- $f|_{\partial X} : \partial X \rightarrow D^2$ is an open book decomposition on ∂X .

We say that f is *concave* if there is a disk $D \subset \text{int } \Sigma$ with

- $f(\partial X) = D$, and
- $f|_{\partial X} : \partial X \rightarrow D$ is an open book decomposition on ∂X .

Finally, f is said to be *flat* if

- $f(\partial X) = \partial \Sigma$, and
- $f|_{\partial X} : \partial X \rightarrow \partial \Sigma$ is a nonsingular fibration.

The fibers of a flat fibration are all closed surfaces, and the boundary ∂X consists of the fibers above $\partial \Sigma$. The fibers of a convex fibration all have boundary, and ∂X is comprised of the fibers above $\partial \Sigma = \partial D^2$, along with

the boundaries of the fibers above $\text{int } D^2$. In contrast, concave fibrations will have both closed fibers and fibers with boundary. Indeed, the fibers above $\text{int } D \subset \Sigma$ will have boundary, while all other fibers will be closed.

Suppose now that $f_1 : X_1 \rightarrow \Sigma$ is a concave fibration, $f_2 : X_2 \rightarrow D^2$ is a convex fibration, and that there is an orientation-reversing diffeomorphism $\phi : \partial X_1 \rightarrow \partial X_2$ which respects the induced open book decompositions. In other words, there is a diffeomorphism $\phi_0 : f_1(\partial X_1) \rightarrow f_2(\partial X_2)$, such that $\phi_0 \circ f_1 = f_2 \circ \phi$. Then (X_1, f_1) and (X_2, f_2) can be glued together to give a fibration $f : X_1 \cup_\phi X_2 \rightarrow \Sigma$ on the closed manifold $X_1 \cup_\phi X_2$.

This gives a very useful method for constructing fibrations on closed 4-manifolds. Indeed, one effective strategy is to divide X into simpler pieces X_1 and X_2 , on which convex and concave fibrations can be constructed. In general these maps will induce different open book decompositions along their common boundary. If, however, these fibrations can be modified so that they agree along $\partial X_1 = \partial X_2$, then they can be glued to give a fibration on all of X . We will discuss approaches to the problem of matching these boundary open book decompositions further in Section 4.5.

4.4 Near-symplectic manifolds and broken fibrations

Lefschetz fibrations are of great interest in 4-manifold topology, in large part due to theorems of Donaldson [10] and Gompf [18] relating them to symplectic 4-manifolds. Indeed, Donaldson proved that any symplectic 4-manifold admits

a *Lefschetz pencil*. That is, there is a finite set of points $B \subset X$ and a Lefschetz fibration $F : X \setminus B \rightarrow \mathbb{C}\mathbb{P}^1$, such that around each point of B the map F is locally modeled by the projectivization map $\mathbb{C}^2 \setminus \{0\} \rightarrow \mathbb{C}\mathbb{P}^1$. Blowing up at the points in B gives an honest Lefschetz fibration, and thus Donaldson's result can be restated by saying that any symplectic 4-manifold admits a Lefschetz fibration over $\mathbb{C}\mathbb{P}^1$ after blow-ups. Gompf proved the converse to this, by showing that any manifold which admits a Lefschetz pencil also admits a symplectic structure.

A similar relationship exists between broken Lefschetz fibrations and *near-symplectic structures*. Let ω be a smooth closed 2-form with $\omega^2 \geq 0$, and set $Z = \{\omega = 0\}$. Then ω is called a *near-symplectic structure* on X if $\omega^2 > 0$ on the complement of Z , and for each point in Z there is a neighborhood U such that the map $U \rightarrow \Lambda^2(T^*U)$ induced by ω has rank 3. This implies that the zero locus Z is a family of embedded circles. Manifolds admitting near-symplectic structures are quite common. Indeed, any closed oriented smooth 4-manifold with $b_2^+(X) > 0$ admits a near-symplectic structure (see [22]).

Analogous to the relationship between Lefschetz pencils and symplectic structures, Auroux, Donaldson, and Katzarkov [4] proved the following: a smooth 4-manifold X admits a near-symplectic structure with zero locus Z if and only if it admits a broken Lefschetz pencil f with round 1-handle singularities along Z , and there is a class $\omega \in H^2(X)$ that evaluates positively on every component of every fiber of f . These structures can be chosen to be compatible, in the sense that if we specify either a near-symplectic structure or broken Lefschetz pencil, then the other object may be chosen so that the regular fibers of the pencil are symplectic away from the singular locus.

4.5 Constructions of fibrations on closed 4-manifolds

Besides establishing a relationship between near-symplectic structures and broken Lefschetz fibrations, Auroux, Donaldson, and Katzarkov also constructed a fibration on S^4 with a single round 1-handle singularity, and no other critical points. As S^4 is clearly not near-symplectic, this raised the question of determining which smooth oriented 4-manifolds admit broken Lefschetz fibrations.

The literature contains a number of results establishing the existence of different fibration structures on closed 4-manifolds, as various authors sought to answer this and related questions. In [13] Etnyre and Fuller proved that after surgery along an embedded circle every smooth closed 4-manifold admits an achiral Lefschetz fibration. Gay and Kirby proved in [16] that every smooth closed 4-manifold admits a broken achiral Lefschetz fibration, while Akbulut and Karakurt strengthened this result in [1] by showing that every closed smooth 4-manifold admits a broken Lefschetz fibration.

The proof of each of these results involves cutting X up into pieces and constructing the desired fibrations on the pieces separately, before regluing. The main differences in their approaches lie in the modifications they make to the fibrations to match the induced open book decompositions. In each approach however, the core argument is the same, relying on machinery from contact topology to ensure that the open book decompositions match before the pieces are reglued.

More precisely, the fibrations are first modified to ensure that both boundary open book decompositions support overtwisted contact structures, and

then to arrange that both of these contact structures are homotopic. By Eliashberg's classification of overtwisted contact structures [12] the two contact structures must then be isotopic, and hence by Giroux's theorem [17] the boundary open book decompositions will agree after some number of positive stabilizations (which can be realized by further modifications to the fibrations). This process is, of course, non-constructive due to its reliance on these deep classification results.

Note that the existence of broken Lefschetz fibrations on arbitrary 4-manifolds had also been proven at the same time independently by both Baykur [5] and Lekili [35], by studying deformations of generic maps near their singularities.

In the case when $b_2^+(X) > 0$ the near-symplectic structure can be used to construct broken Lefschetz fibrations and pencils with additional desired properties. For example, it can be shown that any near-symplectic structure is cohomologous to a near-symplectic form which has connected zero locus, and this can be used to show that in this case X admits a broken Lefschetz pencil with connected fibers, at most one round 1-handle singularity, and that the round 1-handle image is embedded.

Our approach to proving Theorem 1.4.4 will also involve splitting X into pieces, though our convex fibration will be built from the boundary inwards, allowing us to specify the boundary open book ahead of time. This in turn allows us to avoid using deep classification results from contact topology or making the choice of a generic map as in Baykur and Lekili's approaches. Furthermore, our method uses the handle structure of X directly, and hence provides a more concrete geometric approach to the construction of these fi-

brations.

4.6 The topology of broken Lefschetz fibrations

The regular fibers of an (achiral) Lefschetz fibration $f : X \rightarrow \Sigma$ will all be surfaces of the same diffeomorphism type, which we call the *genus of f* . Lefschetz fibrations of genus $g \geq 2$ can be determined entirely by their *monodromy representations*. Let $\Sigma^* \subset \Sigma$ denote the set of regular values of f , and let $p \in \Sigma \setminus \Sigma^*$ be a critical value. If $\gamma \subset \Sigma^*$ is an oriented loop based at $q \in \Sigma^*$ which travels counterclockwise around p and no other critical values, then a trivialization of the bundle over γ induces a diffeomorphism of the fiber F_q above q . This diffeomorphism will be a right-handed (left-handed) Dehn twist if p corresponds to a Lefschetz critical point (anti-Lefschetz critical point respectively). The cycle along which this Dehn twist takes place is called the *vanishing cycle* associated to the critical point. As we approach the critical fiber F_p , the corresponding vanishing cycles in nearby regular fibers shrink down to a single transverse intersection in F_p (see Figure 4.1 where the vanishing cycle is denoted with a dashed line).

Now suppose that $f : X \rightarrow \Sigma$ is a broken fibration, with round 1-handle singularity along an embedded circle C . Suppose that $C' \subset \Sigma$ is the image of C under f , and that C' is embedded. Let p and q be nearby regular points sitting on opposite sides of C' . Suppose for concreteness that $p = (\theta, -1)$ and $q = (\theta, 1)$ for some $\theta \in S^1$ in the coordinate charts described above. Then

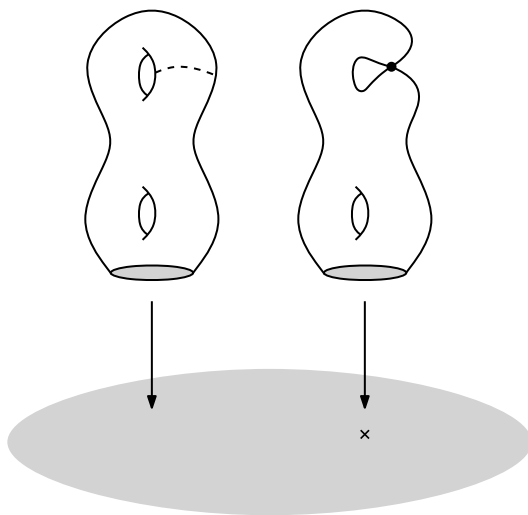


Figure 4.1: Vanishing cycle of Lefschetz critical point

the fiber F_q above q can be obtained from F_p by 0-surgery along a pair of points in F_p . Equivalently, F_p can be obtained from F_q by 1-surgery along a simple closed curve (see Figure 4.2). Indeed, we can think of the coordinate charts describing the round 1-handle singularity as defining an S^1 family of local Morse functions, each with a single index 1 critical point. In particular, the genus of the fiber of a broken fibration changes by ± 1 each time we cross the image of a round 1-handle singularity in Σ .

Now suppose that $f : X \rightarrow D^2$ is a Lefschetz fibration, possibly achiral, possibly broken. Let K be a framed knot in $f^{-1}(\partial D^2) \subset \partial X$, which can be isotoped so that it lies entirely on the interior of a single fiber. Then we can attach a 2-handle along K to yield a new manifold with boundary X' . If we chose the framing along K so that it is one less than the induced fiber framing, then f will extend to a fibration on X' with a new Lefschetz critical point in the newly added 2-handle. If we instead choose K to have framing one greater than the induced fiber framing, f will instead extend to a fibration on X' with

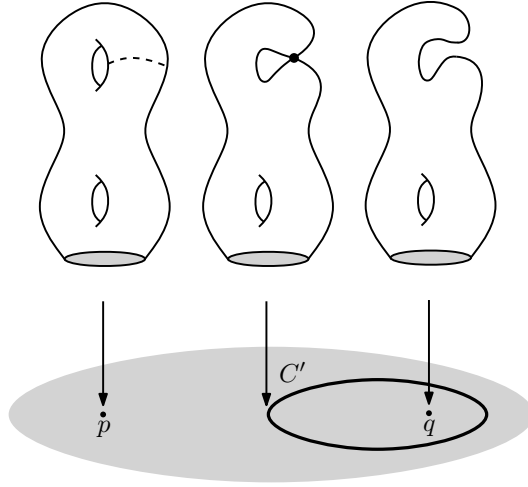


Figure 4.2: Passing a round 1-handle singularity

an additional anti-Lefschetz critical point.

Example 4.6.1. (Achiral Lefschetz fibrations on 2-handlebodies) The first general construction of achiral Lefschetz fibrations on 4-manifolds is due to Harer [19], who showed that every 4-manifold which has a handlebody structure with handles of index ≤ 2 admits a flat achiral Lefschetz fibration over D^2 . We briefly sketch this construction here. For more details see [13].

Fix a handle decomposition on X which has a single 0-handle, and no handles of index ≥ 3 , and let X_1 denote the union of the 0 and 1-handles. Then $X_1 \cong F \times D^2$ for some surface F , which admits the obvious fibration over D^2 with fiber F . The first two figures in Figure 4.3 show handlebody diagrams of X and X_1 , for such a space X . The third figure shows a fiber of the fibration $X_1 \rightarrow D^2$, which is understood to extend over the 1-handles.

In order to extend this fibration over the 2-handles, we must arrange so that each attaching circle lies on a fiber, with framing ± 1 the framing induced by the fiber. Figure 4.4 indicates how this first task can be accomplished

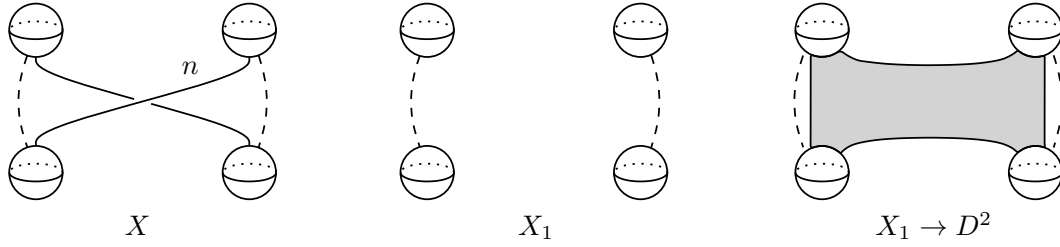


Figure 4.3: Fibration on handles of index 0 and 1

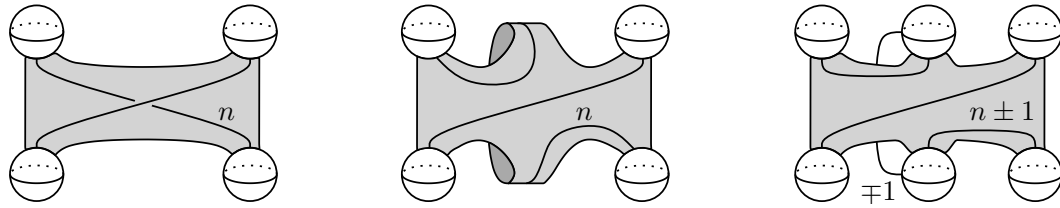


Figure 4.4: Modifying fibration for fiberwise 2-handle attachment

(where we suppress the reference arcs for the 1-handles). Indeed, the double point in the projection of the attaching circle of the 2-handle onto the fiber can be eliminated by adding a band b to the fiber and rerouting the under crossing strand along b as shown in the middle figure. To ensure that this modified surface is the fiber of some map to D^2 , we add an additional 1 and 2-handle canceling pair, and slide the band b over the new 1-handle. The attaching circle of the canceling 2-handle can be isotoped to lie flat on a parallel fiber, and if we chose it to have framing ± 1 (so that the fibration extends over it), then the original 2-handle framing will change as in the rightmost diagram of Figure 4.4. By repeating this procedure, we can ensure that each of the original 2-handles has framing ± 1 the fiber framing, as required.

We now present a handle description for round 1-handle singularities. Suppose again that $f : X \rightarrow D^2$ is a fibration as above, but that we have now chosen two disjoint knots K_1 and K_2 in ∂X , each of which give a section of

f restricted to $f^{-1}(\partial D^2) \subset \partial X$. Then we obtain a new manifold X'' by attaching $S^1 \times D^1 \times D^2$ to ∂X along K_1 and K_2 , by identifying $S^1 \times \{-1\} \times D^2$ and $S^1 \times \{1\} \times D^2$ with tubular neighborhoods of K_1 and K_2 respectively. In this case the fibration f will extend to X'' , with a single round 1-handle singularity along $S^1 \times \{0\} \times \{0\}$. Indeed, the knots K_1 and K_2 intersect each of the boundary fibers in a pair of points, which specify the locations of the 0-surgeries that take place as we pass the round 1-handle image. Note that this also explains the choice of name for critical points of this type, as $S^1 \times D^1 \times D^2$ can be thought of as an S^1 -family of 3-dimensional 1-handles $D^1 \times D^2$, which are attached to X fiberwise along the boundary. Alternatively, we can split $S^1 \times D^1 \times D^2$ into a 4-dimensional 1-handle and 2-handle pair, where the 2-handle runs over the 1-handle twice geometrically, but zero times algebraically.

The monodromy of the fibration outside this new round 1-handle singularity will depend on the framings of the tubular neighborhoods of K_1 and K_2 , or alternatively, on the framing k of the 2-handle in the 4-dimensional handle pair description. Indeed, suppose that F is the fiber of the fibration f before attaching the round 1-handle, and that the monodromy around the boundary ∂D^2 is given by a map $\varphi : F \rightarrow F$. Then adding the new round 1-handle changes the fibers along the boundary by replacing two disks D_1 and D_2 in F with $S^1 \times [0, 1]$. The new monodromy will be given by the restriction of φ to $F \setminus (D_1 \cup D_2)$, with k Dehn twists along the cycle $S^1 \times \{\frac{1}{2}\}$.

We will also sometimes refer to round 2-handles, which are the product of a 3-dimensional 2-handle with S^1 . These are, of course, just upside-down round 1-handles, and will not warrant any further discussion.

Example 4.6.2. The next example we consider will involve constructing a concave broken fibration $f : S^2 \times D^2 \rightarrow S^2$, which has a single round 1-handle singularity, and no other critical points. This construction is originally due to Auroux, Donaldson, and Katzarkov [4], as part of their construction of a broken Lefschetz fibration on S^4 . It can easily be generalized to construct a similar fibration on $F \times D^2$ for any closed orientable surface F , and will be necessary for our proof of Theorem 1.4.4.

We begin by identifying the target of the projection $\text{pr}_2 : S^2 \times D^2 \rightarrow D^2$ with the northern polar cap in S^2 . This defines a fibration of $S^2 \times D^2$ with fiber S^2 over this region (see the bottom left diagram in Figure 4.5). Expressing $S^2 \times D^2$ with the usual handlebody diagram (top left Figure 4.5), we can add a 1-handle and 0-framed 2-handle to this diagram, as in the top middle diagram. Taken together, these two handles can be interpreted as a round 1-handle, which is attached to $S^2 \times D^2$ along two sections of the existing fibration restricted to the boundary. We can thus extend this fibration over the round 1-handle, giving a fibration over the northern hemisphere with a round 1-handle singularity over the arctic circle. Fibers between the equator and arctic circle will be obtained from the polar fibers by 0-surgery, and hence will be tori. Note that the fibration we have constructed so far is flat along its boundary.

Finally, we add an additional 2-handle H_2 , and a 3-handle H_3 to our diagram (top right, Figure 4.5). The attaching circle of H_2 is a section over the boundary, and hence the fibration can be extended over $H_2 \cong D^2 \times D^2$, by projecting it to the southern hemisphere (with fiber D^2). The resulting fibration is concave. The page of the boundary open book decomposition is

a torus with a single hole (which resulted from attaching the 2-handle H_2), while its binding will be the belt-sphere of H_2 .

The attaching sphere of the new 3-handle H_3 is arranged so that it intersects the binding at its north and south poles, and so that it intersects each page in a properly embedded arc. The fibration can then be extended across H_3 , resulting in no new critical points. This extension changes the D^2 fibers over the southern hemisphere by adding a 2-dimensional 1-handle, yielding annular fibers. On the other hand, the pages of the boundary open book change by the *removal* of a neighborhood of a properly embedded arc (the intersection of the original page with the attaching sphere of H_3), yielding disconnected pages. Each of these pages consists of a D^2 component and punctured torus component.

The result of all these additions is thus a concave broken fibration as depicted in the bottom right diagram of Figure 4.5, with a single round 1-handle singularity, and no Lefschetz or anti-Lefschetz critical points. Moreover, after sliding the 0-framed 2-handle off of the 1-handle, we find that the added 1,2, and 3-handles all form canceling pairs. Hence the total space of our fibration is diffeomorphic to $S^2 \times D^2$.

4.7 Replacing anti-Lefschetz critical points

We end our general discussion of broken achiral Lefschetz fibrations by briefly describing a method due to Lekili [35] for removing anti-Lefschetz critical points from a given fibration. This move was introduced during his study of *wrinkled fibrations*, which are a class of fibrations with certain cusp points

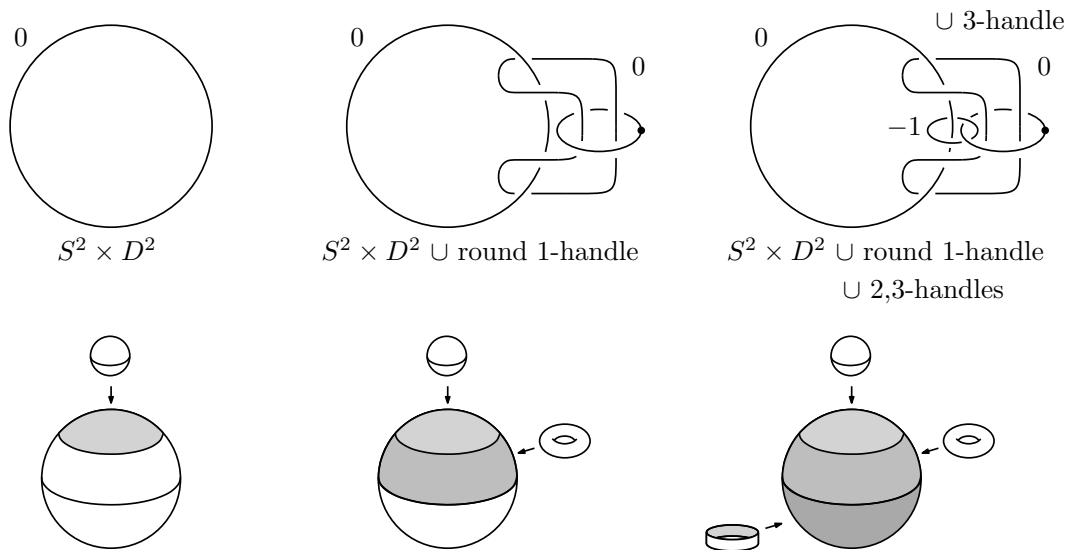


Figure 4.5: Concave broken fibration on $S^2 \times D^2$.

allowed along the round 1-handles singularities. The replacement can be described as a local perturbation near the anti-Lefschetz point, resulting first in a wrinkled fibration, then back to a broken fibration with a new round 1-handle singularity and three new Lefschetz critical points in place of the original (anti-Lefschetz) critical point. Baykur also gave a description of this replacement in terms of handle diagrams as an appendix to [35]. As both descriptions are somewhat complicated, we will only discuss this move in terms of the vanishing cycles of the affected critical points.

The replacement is outlined in Figure 4.6, where only a local picture of the fibration is shown. On the left is a single anti-Lefschetz critical point, with vanishing cycle indicated in the fiber. The fibration map can be modified in a neighborhood of this critical point so that it is instead as depicted on the right-hand side of Figure 4.6, with three Lefschetz critical points and a new round 1-handle singularity. Here the fiber shown is assumed to be above a

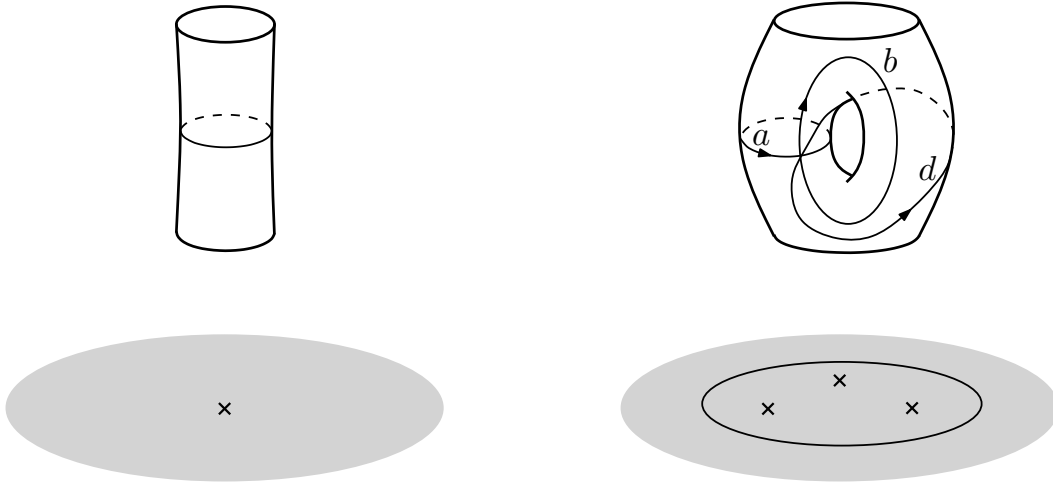


Figure 4.6: Replacing an anti-Lefschetz critical point

point interior to the triangle formed by the three isolated critical values. The vanishing cycles of these Lefschetz critical points can be described in terms of the three labeled cycles shown in the diagram. In counterclockwise order these vanishing cycles are given by $a - d$, $d - b$, and $b - a$. Denote the corresponding critical values by α , δ , and β , respectively, and let C denote the image of the round 1-handle singularity.

Suppose now that we start at the center fiber shown in Figure 4.6 and, moving outwards, cross over C . As we pass over this round 1-handle singularity image, the fiber will change by a 1-surgery (corresponding to the addition of a round 2-handle). The circle along which we perform the 1-surgery depends, however, on which way we exit. For example, if we choose a path that only crosses the edge $\beta\alpha$ before crossing C as in Figure 4.7, then the corresponding 1-surgery will take place along a . Exiting through the edge $\alpha\delta$ will result in a 1-surgery along d , while exiting through $\delta\beta$ will yield surgery along the loop b .

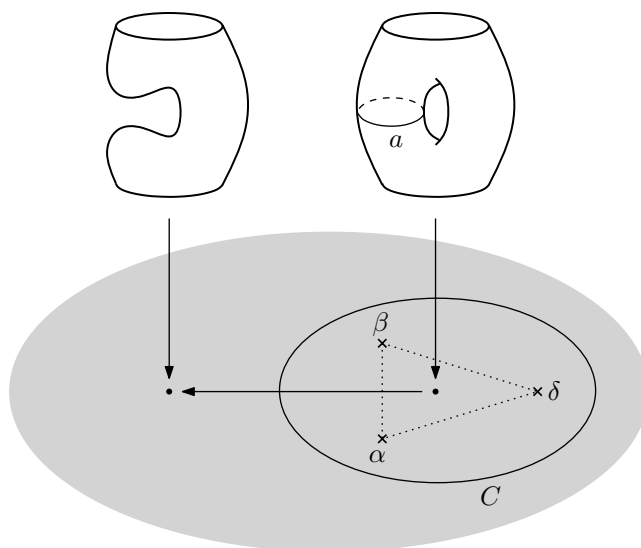


Figure 4.7: Surgery cycle in the fiber for Lekili's replacement

We conclude this section with two observations which will be important in what follows. First, note that the three vanishing cycles we introduced during this local modification are nontrivial in the homology of the fiber, regardless of whether the original anti-Lefschetz vanishing cycle was or not. Second, suppose that E is the image of another Lefschetz or anti-Lefschetz critical point, sitting outside of C . Suppose we choose a path μ from E to a point on the round 1-handle image C . Crossing C along this path from the outside results in a 0-surgery on the fiber, at a pair of points which can be assumed to be disjoint from the vanishing cycle associated to E . We can thus modify the fibration in a neighborhood of μ so that E is moved to the inside of C . By a similar argument, if we have replaced a number of these anti-Lefschetz critical points in this way, and hence have obtained multiple circles corresponding to new round 1-handles, then they can all pass over each other to be arranged as a sequence of nested circles.

Chapter 5

Broken Lefschetz fibrations via branched coverings

In this section we present the proofs of Theorems 1.4.3 and 1.4.4. The proof of Theorem 1.4.3, which involves finding a convex broken Lefschetz fibration on X with $\partial X \neq \emptyset$ connected, relies on the construction of a branched covering $H : X \rightarrow D^2 \times D^2$ one handle at a time, after which we use Theorem 1.4.1 to arrange the branch locus of H as a braided surface with caps. When composed with the projection to D^2 , this map will give the desired convex fibration on X . We can then appeal to Lekili's *wrinkling* move to eliminate any anti-Lefschetz critical points we may be left with. Theorem 1.4.3 is then combined with constructions of concave fibrations due to Gay and Kirby [16] (see also Example 4.6.2), to build broken Lefschetz fibrations on arbitrary closed oriented 4-manifolds, thus proving Theorem 1.4.4.

5.1 Singular branched coverings

We will need to consider two maps which will serve as local models of the types of allowable singularities of branched coverings we consider. We define a 3-fold simple branched covering $h_T : \partial(D^2 \times D^2) \rightarrow \partial(D^2 \times D^2)$ as follows. Let $\partial_1 \cup \partial_2$ and $\partial'_1 \cup \partial'_2$ denote decompositions of the source and target $\partial(D^2 \times D^2)$ into solid tori as above. Let $K \subset \partial'_1$ be the closure of the colored braid on the far right of Figure 5.2 (which yields a trefoil). Then define h_K on ∂_1 as a simple 3-fold irregular covering of ∂'_1 branched along K , and on ∂_2 as a 3-fold unbranched covering of ∂'_2 . Here the fibrations are chosen to match smoothly along the boundary, and to respect the natural product structures of the ∂_i and ∂'_i .

Then define $h_C : D^2 \times D^2 \rightarrow D^2 \times D^2$ by setting

$$h_C(x) = \|x\| \cdot h_K \left(\frac{x}{\|x\|} \right)$$

for $\|x\| \neq 0$, and $h_C(0, 0) = (0, 0)$ (where we are viewing D^2 as the unit disk in \mathbb{C}). Clearly h_C is continuous and is a smooth 3-fold branched covering away from the origin. Singularities of a branched covering locally modeled by h_C will be called *cusp singularities*. The branch locus of h_C is the cone over the trefoil $T \subset \partial'_1$ with cone point at the origin (which we refer to as a *cusp singularity* of the branch locus). Notice that $\text{pr}_2 \circ h_C = \text{pr}_2$.

Let $h_N : D^4 \amalg D^4 \rightarrow D^4$ be the simple 4-fold branched covering of D^4 , where each component in the domain is mapped to the base as a 2-fold branched covering branched over an unknotted disk. The branch loci are

arranged so that they meet transversely in a single interior point (which we refer to as a *node singularity* of the branch locus). Note that h_N restricts on the boundary to a 4-fold branched covering $S^3 \amalg S^3 \rightarrow S^3$ with branch locus the Hopf link. Points around which a branched covering is modeled by h_N will be called *node singularities*.

5.2 Constructing the branched coverings

Suppose now that we have a smooth 4-manifold X , and that a choice of open book decomposition $\lambda : \partial X \rightarrow D^2$ with connected page and binding has been fixed. We will construct a branched covering $H : X \rightarrow D^2 \times D^2$ as described above, so that the restriction of $\text{pr}_2 \circ H$ to ∂X equals λ .

Remark Since $D^2 \times D^2$ is a manifold with corners, the map H will not be a local diffeomorphism along the preimage of the corners. We can assume however that H is smooth (away from all cusp singularities), with $\text{pr}_2 \circ H$ regular away from its branch locus. Indeed, we could proceed by constructing a smooth branched covering $\tilde{H} : X \rightarrow D^4$ handle-by-handle as explained below, and then choosing a smooth homeomorphism $\eta : D^4 \rightarrow D^2 \times D^2$, with $\text{pr}_2 \circ \eta : D^4 \rightarrow D^2$ a regular map (such a η is not difficult to construct). The map H would then be defined as $H = \eta \circ \tilde{H}$. To simplify the discussion in what follows, we will refrain from making any further mention of these considerations.

Proposition 5.2.1. *The open book decomposition $\lambda : \partial X \rightarrow D^2$ factors as $\partial X \xrightarrow{h} \partial(D^2 \times D^2) \xrightarrow{\text{pr}_2} D^2$, where h is an irregular simple 4-fold covering*

branched along a closed braid $L \subset \partial_1$. Moreover, h can be assumed to have been obtained by adding a single trivial sheet to a 3-fold branched covering $\partial X \rightarrow \partial(D^2 \times D^2)$.

Proof. Let $Y_1 = \lambda^{-1}(\partial D^2)$ and $Y_2 = \overline{\lambda^{-1}(\text{int } D^2)}$. We begin by constructing a 3-fold covering $h_0 : \partial X \rightarrow S^3$ with the desired properties, after which we add the trivial sheet. We construct h_0 piecewise as

$$h_1 : Y_1 \rightarrow \partial_1 \quad \text{and} \quad h_2 : Y_2 \rightarrow \partial_2$$

which will match along $\partial Y_1 = \partial Y_2$.

Then there is a compact surface Σ with connected, non-empty boundary, and a diffeomorphism $\phi : \Sigma \rightarrow \Sigma$ which is the identity near $\partial \Sigma$, so that Y_1 can be identified with the mapping torus $M_\phi = ([0, 1] \times \Sigma)/(0, x) \sim (1, \phi(x))$ of ϕ . Note that Σ will be diffeomorphic to the page of λ , and the surface $\lambda^{-1}(s)$ is identified with $\{s\} \times \Sigma \subset M_\phi$ for any $s \in \partial D^2 = \mathbb{R}/\mathbb{Z}$.

Let g denote the genus of Σ , and let $\tau : \Sigma \rightarrow D^2$ be the irregular 3-fold covering shown in Figure 5.1, which is branched over $2g + 2$ points. Here the map τ is given by “folding” Σ along the two dotted lines in the figure (for a more precise description see the covering constructed in [21], from which we obtain τ by removing a disk).

By [34] the map $\phi : \Sigma \rightarrow \Sigma$ is isotopic to a sequence of Dehn twists along the $2g + 1$ curves b_i in the figure. By [21] each of the Dehn twists along the b_i curves is isotopic to the lift of a diffeomorphism of D^2 . Thus there exist diffeomorphisms $\phi_0 : \Sigma \rightarrow \Sigma$ and $\phi_1 : D^2 \rightarrow D^2$ such that ϕ_0 is isotopic to ϕ , and $\tau \circ \phi_0 = \phi_1 \circ \tau$. We thus obtain a fiberwise branched covering map h_1

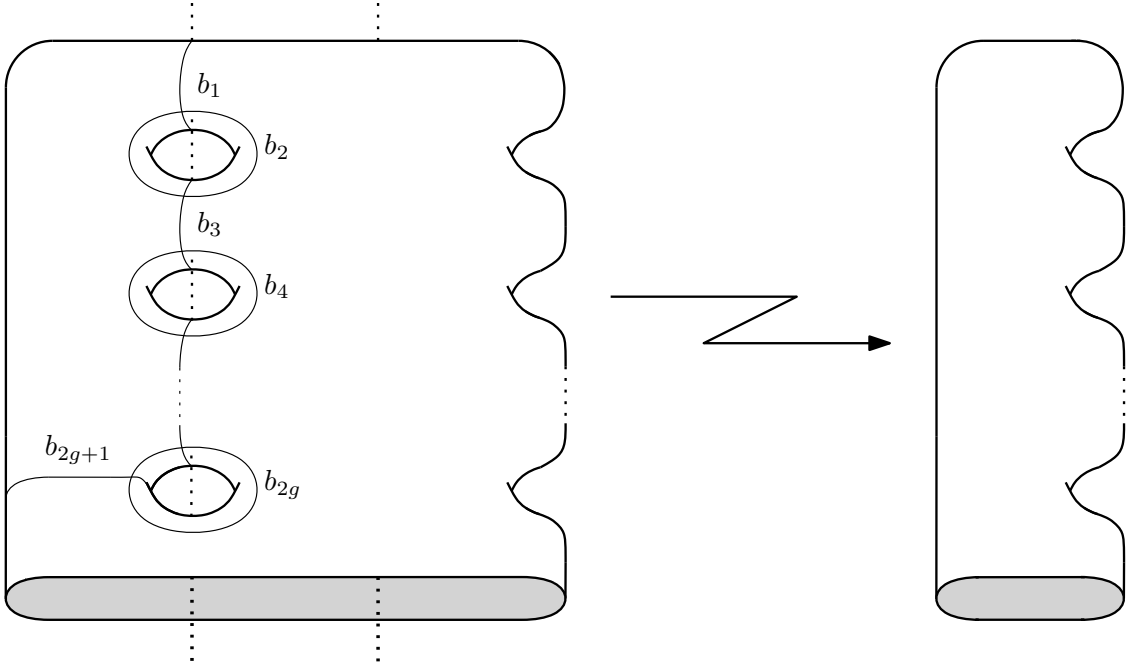


Figure 5.1: 3-fold branched cover $\Sigma \rightarrow D^2$

from $M_{\phi_0} \cong Y_1$ to $M_{\phi_1} \cong \partial_1$ as required.

To define $h_2 : Y_2 \rightarrow \partial_2$, first set $h_2 \equiv h_1$ on $\partial Y_2 = \partial Y_1$, and extend as a 3-fold covering to the rest of Y_2 in such a way that $\text{pr}_2 \circ h_2 = \lambda|_{Y_2}$.

Using the construction above it is easy to describe the required 4-fold cover h . We can obtain a 4-fold cover $Y_1 \rightarrow \partial_1$ from h_1 at the cost of adding an unknotted circle of branch points in ∂_1 , which is unlinked from the branch locus of h_1 . A map $Y_2 \rightarrow \partial_2$ can then be constructed as above to match along the boundary. Gluing these two 4-fold covering maps (branched and unbranched respectively) gives h . \square

Lemma 5.2.2. *There is a simple 4-fold cover $H : X \rightarrow D^2 \times D^2$, possibly with cusp or node singularities, such that $H|_{\partial X} \equiv h$ as maps from ∂X to*

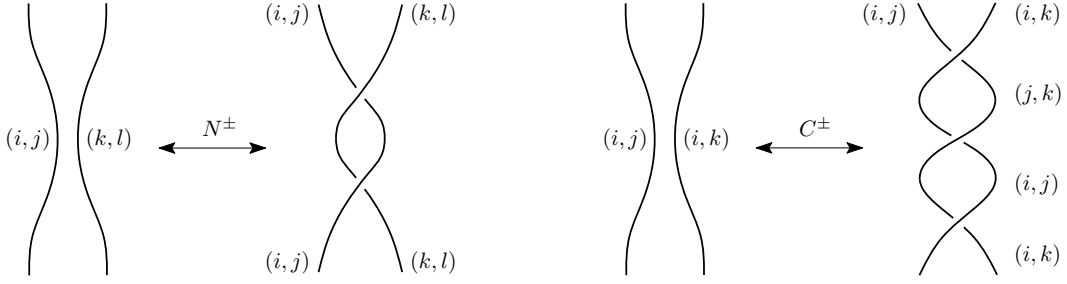


Figure 5.2: N^\pm and C^\pm branched covering moves

$\partial(D^2 \times D^2)$, and so that away from the images of any cusp or node singularities the branch locus of H is an embedded orientable surface.

Proof. Fixing a relative handle decomposition of $(X, \partial X)$ with a single 4-handle, let X_0 denote the union of $\partial X \times [0, 1]$ with the 1 and 2-handles, and X_1 the union of the 3-handles and 4-handle. By taking the product of h with the identity on $[0, 1]$, we get a covering of $H_0 : \partial X \times [0, 1] \rightarrow \partial(D^2 \times D^2) \times [0, 1]$ branched along the product of the branch locus of h with $[0, 1]$. After isotopy near $\partial X \times \{1\}$, we can assume that the single loop in the branch locus of $H_0|_{\partial X \times \{1\}}$ corresponding to the trivial sheet lies in a 3-ball which is disjoint from the attaching regions of the 1 and 2-handles.

By Lemma 6.1 of [7] and Theorem 4.4 of [11], the branched covering H_0 can be extended across the 1 and 2-handles of X to give a 4-fold simple branched covering $H_0 : X_0 \rightarrow \partial(D^2 \times D^2) \times [0, 1]$. For each 1 or 2-handle of X , we must add a 0 or 1-handle respectively to the branch locus in $\partial(D^2 \times D^2) \times [0, 1]$. By applying the covering moves in [3] we can assume that the branch locus is orientable.

Similarly, let $H_1 : D^4 \rightarrow D^2 \times D^2$ be a simple 4-fold covering branched along three properly embedded unknotted disks. Identifying the unique 4-

handle with D^4 , we assume that the boundaries of these disks lie in disjoint 3-balls which avoid the regions where the 1-handles (or upside-down 3-handles) attach to D^4 . We can extend H_1 to a 4-fold simple covering $H_1 : X_1 \rightarrow D^2 \times D^2$, branched along a collection of properly embedded disks.

Now ∂X_0 consists of two components, one of which corresponds to ∂X , while the other is the result of performing surgeries to ∂X along the attaching regions of the 1 and 2-handles. Denote this latter component by $\partial_+ X_0$. Clearly $\partial_+ X_0 \cong \partial X_1$, while $H_0|_{\partial_+ X_0}$ and $H_1|_{\partial X_1}$ are simple 4-fold branched coverings of $\partial_+ X_0 \cong \partial X_1$ over $\partial(D^2 \times D^2)$. By construction both of these coverings arise from 3-fold branched coverings by the addition of a trivial sheet. By [40] then there is a finite sequence of C^\pm and N^\pm moves to the branch locus in S^3 (see Figure 5.2), which transforms the covering $H_0|_{\partial_+ X_0}$ to $H_1|_{\partial X_1}$.

It is easy then to construct a branched covering $\partial_+ X_0 \times [0, 1] \rightarrow S^3 \times [0, 1]$ which restricts to $H_0|_{\partial_+ X_0}$ on $\partial_+ X_0 \times \{0\}$ and $H_1|_{\partial X_1}$ on $\partial_+ X_0 \times \{1\}$, which has one cusp singularity or node singularity respectively for each C^\pm or N^\pm move performed. Indeed, each move is realized by boundary summing with the local model of h_C or h_N in a neighborhood of the move, matching the maps along the gluing region. The desired branched covering H is then obtained by gluing the above constructions in the obvious way. \square

We will denote the branch locus of H as B_H . It is an orientable surface with cusp and node singularities.

5.3 Constructing the broken fibration

We now proceed to prove Theorems 1.4.3 and 1.4.4.

Proof of Theorem 1.4.3. By Corollary 1.4.2, we can assume that B_H is a braided surface with caps in $D^2 \times D^2$ (notice that the node and cusp singularities can be treated exactly as the saddle points in the proof of Theorem 1.4.1). Away from the preimages of the critical points of $\text{pr}_2|_{B_H}$, the composition $f = \text{pr}_2 \circ H$ is a regular map. By [36] f has a Lefschetz (resp. anti-Lefschetz) critical point for every positive (resp. negative) branch point of $\text{pr}_2|_{B_H}$.

To see that the fold lines of B_H along the boundaries of the caps give round 1-handle singularities, note that along these fold lines B_H is locally embedded as $\mathbb{R}^2 \rightarrow \mathbb{R}^2 \times \mathbb{R}^2$, by $(s, r) \mapsto (0, r, s, r^2)$. Furthermore, near nonsingular points of B_H , H can be written in complex coordinates as $(u, v) \mapsto (u^2, v)$, where B_H is given locally by $u = 0$. Combining these two local models yields a map of the required local form. Furthermore, the folds of B_H have been pushed out so that they lie above a neighborhood of the boundary of D^2 , so that their images form a collection of concentric circles which enclose the Lefschetz and anti-Lefschetz critical values.

We now must deal with the cusp and node singularities in B_H . Notice first that since the two strands of B_H involved in a node singularity correspond to simple branching along disjoint pairs of sheets of the covering H , the node singularities project to regular values of the map f . Near a cusp singularity, we can assume that the map H is given by the 3-fold simple covering h_C , with an extra trivial sheet. Since $\text{pr}_2 \circ h_C = \text{pr}_2$, the map f will also be regular in such a neighborhood.

Clearly Properties 1 and 5 of the theorem will hold, from our construction of f and the corresponding property of braided surfaces with caps. To see that Property 3 holds, note that as we move inwards from the boundary towards

the center of the base D^2 , for every round 1-handle image we pass we will change the fiber by 0-surgery on two points, which increases the genus of the affected component by +1. This is due to the fact that as we pass each round 1-handle images, we increase the number of branch points in the fiber by +2. Since the fibers over ∂D^2 are assumed to be connected, every fiber of f will likewise be connected.

We now show that all vanishing cycles are nontrivial in the homology of the fiber F over $0 \in D^2$ (which we assume to be regular). Recall that restriction of $\text{pr}_2 : D^2 \times D^2 \rightarrow D^2$ to B_H is a branched covering away from the fold lines. If $p \in X$ is a Lefschetz or anti-Lefschetz critical point of f , then $\text{pr}_2|_{B_H} : B_H \rightarrow D^2$ will have a simple branch point above $f(p)$ (at $H(p)$). Then the monodromy map around a small loop enclosing the point $f(p)$ and no other critical values will act on the set $(\text{pr}_2|_{B_H})^{-1}(0) = \{q_1, \dots, q_m\}$ by swapping two points, say q_1 and q_2 , and fixing the other $m - 2$ points. Choose an embedded arc γ in $D^2 \times \{0\}$ connecting q_1 and q_2 . Note that H restricts to a branched covering $H|_F : F \rightarrow D^2 \times \{0\}$, and that γ will lift to a simple closed curve $\tilde{\gamma}$ in the fiber F , which represents the vanishing cycle associated to p , along with disjoint arcs γ_1, γ_2 . Then the restriction of H to $F \setminus (\tilde{\gamma} \cup \gamma_1 \cup \gamma_2)$ gives a branched covering

$$F \setminus (\tilde{\gamma} \cup \gamma_1 \cup \gamma_2) \rightarrow (D^2 \times \{0\}) \setminus \gamma.$$

If $\tilde{\gamma}$ disconnected F , then each component of $F \setminus (\tilde{\gamma} \cup \gamma_1 \cup \gamma_2)$ would also be a branched cover of $(D^2 \times \{0\}) \setminus \gamma$, and would thus have nonempty boundary. But by our assumption on the boundary open book decomposition, ∂F is

connected, and hence $\tilde{\gamma}$ does not separate F .

Finally, using Lekili's wrinkling move (see Section 4.7) we can replace any anti-Lefschetz critical points by new Lefschetz and round 1-handle singularities. It remains only to show that the result of such a replacement factors through a branched covering of $D^2 \times D^2$.

Let $p \in X$ be an anti-Lefschetz critical point of f , and choose small disks D, D' (thought of as sitting in the first and second factor of $D^2 \times D^2$ respectively), such that $D \times D'$ is a small neighborhood of $H(p) \in D^2 \times D^2$. Note that $H(p)$ will lie on B_H , the branch locus of H , and will be a negative branch point of the map $\text{pr}_2|_{B_H} : B_H \rightarrow D^2$. The disks D and D' can be chosen so that $B_H \cap (D \times D')$ is given by $z = w^2$ for some orientation-reversing complex coordinates (z, w) on $D \times D'$ centered at $H(p)$. Hence $B_H \cap \partial(D \times D')$ will be a closed braid in $D \times \partial D'$ of index 2 with a single negative twist.

The preimage $H^{-1}(D \times D')$ will consist of three components, two of which are mapped homeomorphically onto $D \times D'$, while the third is mapped as a 2-to-1 covering of $D \times D'$ branched along $(D \times D') \cap B_H$. Denote this latter component by V .

Every disk of the form $D \times \{q\}$, for $q \in D' \setminus \{f(p)\}$, will intersect the branch locus B_H in precisely two points, and hence will lift to an annulus under the degree 2 branched cover $H|_V : V \rightarrow D \times D'$. Thus $f|_V : V \rightarrow D'$ is an achiral Lefschetz fibration, with regular fiber an annulus and a single critical point which is anti-Lefschetz (see the left-hand side of Figure 4.6).

Lemma 5.3.1. *There is a 2-fold branched covering map $G : V \rightarrow D \times D'$ whose branch locus is a braided surface with a single cap, and three positive*

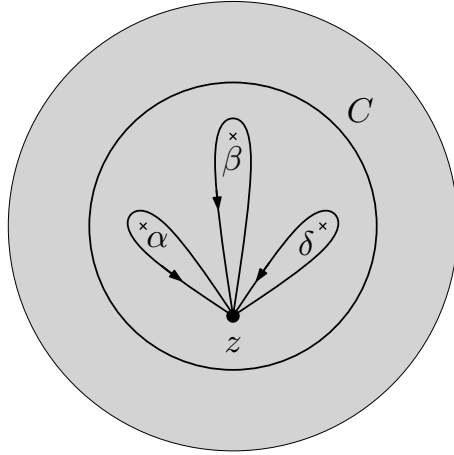


Figure 5.3: Loops c_α, c_β , and c_δ around critical values in D' .

branch points. Moreover, the restrictions $G|_{\partial V}$ and $H|_{\partial V}$ agree.

Proof. Double covers of $D \times D'$ branched along embedded surfaces are determined by their branch loci, and hence it will suffice to describe G in terms of its branch locus $B_G \subset D \times D'$. Choose four points α, β, δ and z in the interior of D' , and choose loops c_α, c_β , and c_δ based at z which encircle the other three points in the counterclockwise direction, as in Figure 5.3. Choose a circle $C \subset D'$ which encircles the loops c_α, c_β , and c_δ , and which is parallel to $\partial D'$.

We define B_G by first describing its intersection with the torus $D \times c_\alpha$. Indeed, we define $B_G \cap (D \times c_\alpha)$ to be the closed braid in $D \times c_\alpha$ obtained as the closure of the braid in Figure 5.4. Likewise, we define the intersection of B_G with $D \times c_\delta$ and $D \times c_\beta$ as the closures of the braids in Figures 5.5 and 5.6 respectively. In each figure, the braids are taken to both start and finish at $B_G \cap (D \times \{z\})$, and the bottom to top orientation is understood to correspond with the counterclockwise orientation of the c curves.

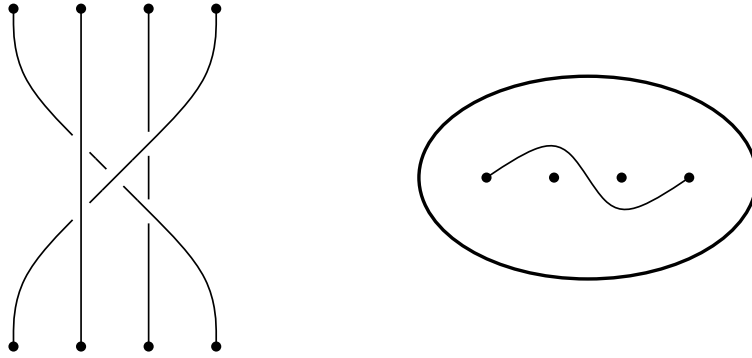


Figure 5.4: Braid monodromy around α , and associated braid twist arc

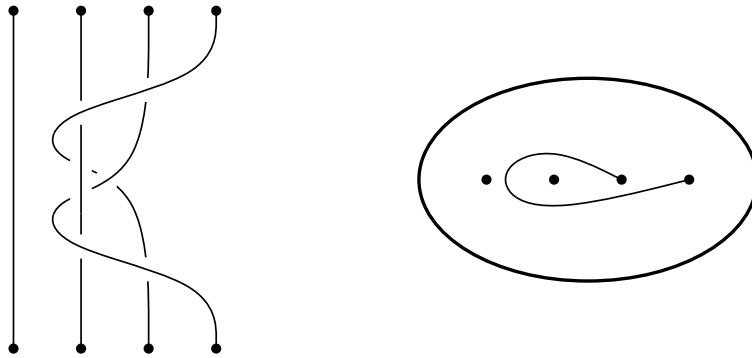


Figure 5.5: Braid monodromy around δ , and associated braid twist arc

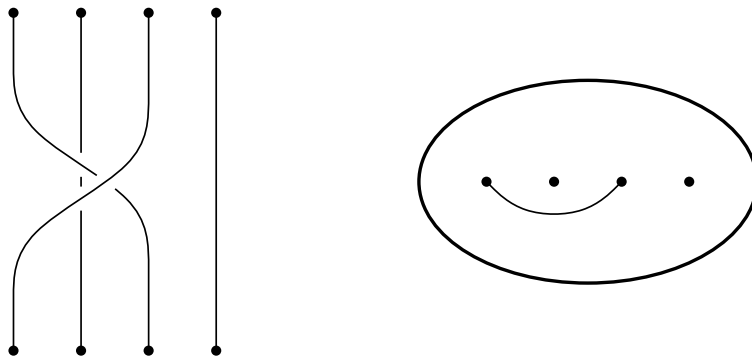


Figure 5.6: Braid monodromy around β , and associated braid twist arc

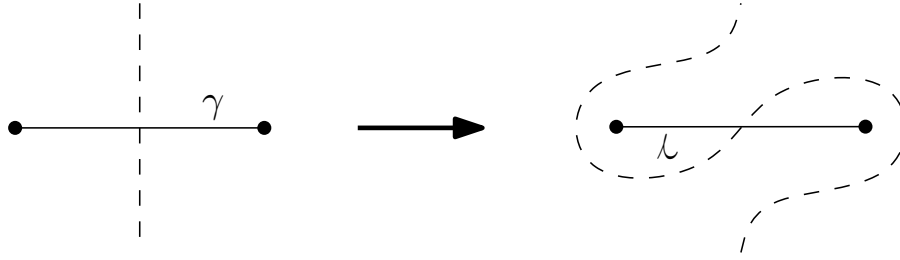


Figure 5.7: Positive braid twist along the arc γ , with dotted arc for reference

Now suppose that p_1, \dots, p_k are points in D . Then any braid in $D \times [0, 1]$ with endpoints at $\{p_1, \dots, p_k\} \times \{0\}$ and $\{p_1, \dots, p_k\} \times \{1\}$ induces a homeomorphism of D which fixes $\{p_1, \dots, p_k\}$ setwise. Note that in the case of the braid $B_G \cap (D \times c_\alpha)$, the associated homeomorphism of D is given by a single positive braid twist (see Figure 5.7). Hence, we can extend B_G across the disk bounded by c_α as a braided surface with a positive branch point above $\alpha \in D$. Likewise, we can extend B_G across the disks bounded by c_β and c_δ , so that it also has positive branch points above β and δ .

Now, suppose that around $C \subset D'$ we have embedded a tubular neighborhood $C \times [-1, 1]$. For each $t \in [-1, 1]$, let $C_t = C \times \{t\}$, and assume that C_{-1} lies inside the disk bounded by $C = C_0$. Then we can extend B_G over the entire disk bounded by C_{-1} , so that it is a braided surface with (positive) branch points only over α, β , and $\delta \in D'$. The boundary of this newly extended surface braid B_G will be a closed braid in $D \times C_{-1}$, which is the product of the three braids in Figures 5.4-5.6 (traveling around c_α, c_δ , and c_β in that order), and is depicted in the top of Figure 5.8. Notice that after taking the closure, the two topmost strands (in starting and finishing position) will bound an annulus A which is otherwise disjoint from the rest of the braid.

Then as we let t go from -1 to 0 , we can define $B_G \cap (D \times C_t)$ by starting

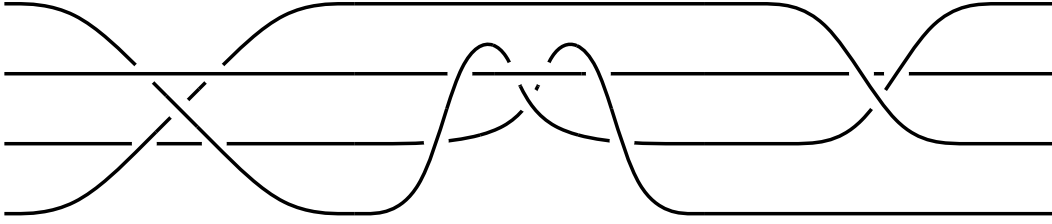


Figure 5.8: Braid whose closure yields $B_G \cap (D \times C_{-1})$

with $B_G \cap (D \times C_{-1})$, and allowing these two strands to merge into a single strand in $B_G \cap (D \times C_0)$, before vanishing when $t > 0$ (see Figure 5.9, where the annulus A is shaded in). Hence $B_G \cap (D \times C_t)$ will have index 4 for $t < 0$, index 3 for $t = 0$, and index 2 for $t > 0$. This yields a fold circle (the boundary of a cap) in the surface B_G sitting above $C \in D'$. We then extend B_G to a braided surface with caps over all of D' , with no additional critical points. Thus B_G will have precisely one cap, and three positive branch points.

Now the surface $B_G \subset D \times D'$ defines a branched covering $G : V_G \rightarrow D \times D'$, with total space V_G . Note that we can arrange B_G so that along $\partial(D \times D')$ it agrees with $B_H \cap \partial(D \times D')$, and hence ∂V_G is diffeomorphic to $\partial V \cong S^3$. Furthermore, the composition $f_G = \text{pr}_2 \circ G$ is a broken Lefschetz fibration with three Lefschetz critical points whose images lie inside the image of the only round 1-handle singularity. By Lekili's substitution, V also admits a broken Lefschetz fibration with a similar configuration of critical points. If we can show that in both fibrations the monodromy around the Lefschetz critical points agree, and that the round 1-handles are attached in the same way, then we will have that $V \cong V_G$.

Denote by Σ_z the preimage of the disk $D \times \{z\}$ under the map G . It is a twice punctured torus, and will be a fiber of the fibration f_G . By [7]

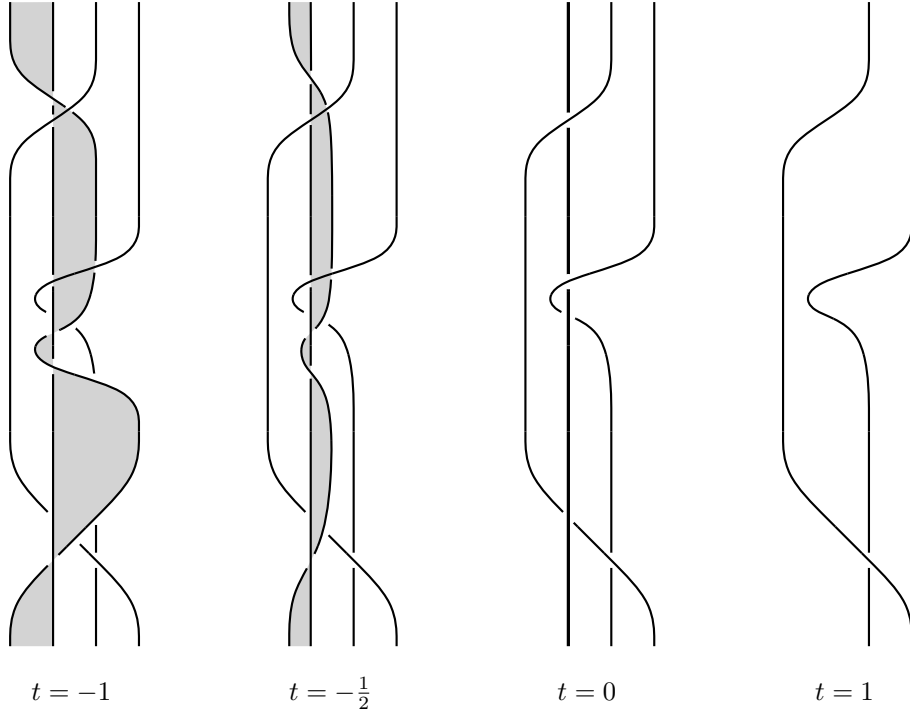


Figure 5.9: Merging strands to give fold line

we can assume that the restriction of G to the fiber Σ_z will be the covering $\phi : \Sigma_z \rightarrow D \times \{z\}$ depicted in Figure 5.10, which is induced by 180° rotation around the axis shown. The monodromy of f_G around the curves c_α , c_δ , and c_β will be lifts under ϕ of the homeomorphisms of $D \times \{z\}$ induced by the braids in Figures 5.4-5.6. The arc on the right-hand side of Figure 5.4 lifts to the cycle $a - d$ (see Figure 4.6 for the orientations), and a positive braid twist along it lifts to a positive Dehn twist. Likewise the arcs in Figures 5.5 and 5.6 lift to cycles $d - b$ and $b - a$ respectively, and the positive braid twist homeomorphisms lift to positive Dehn twists along these cycles. Thus the monodromy around the critical points of f_G agrees with the monodromy in Lekili's replacement fibration in Section 4.7. Thus the total spaces of both fibrations restricted to disks inside the round 1-handle images are diffeomorphic.

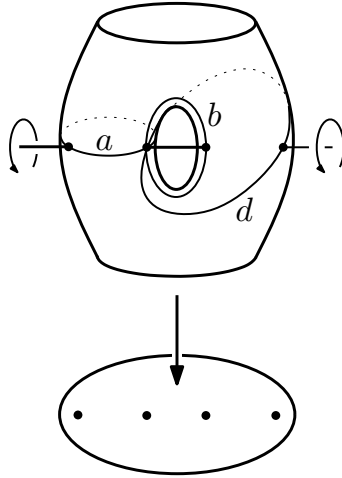


Figure 5.10: Branched covering $\phi : \Sigma_z \rightarrow D \times \{z\}$

Finally, if we lift the annulus A in $D \times C_{-1}$ (depicted on the right in Figure 5.9) we obtain a family of cycles in the fibers above the circle C_{-1} , one cycle on each fiber. Looking at the fibers above C_t as t ranges from -1 to 0 , we see that as A shrinks to a single loop, these cycles each shrink to a point in the fibers. Passing the circle C , we observe fiberwise 1-surgeries on each of the fibers, corresponding to the attachment of a round 2-handle (an upside-down round 1-handle). Thus, starting at z , if we cross C via a path passing between α and β the corresponding 1-surgery will be along a . This agrees with Lekili's description, and hence the round 2-handles attachments are isotopic in both fibrations. As the round handle framings are determined by the monodromy inside C (which we verified matches Lekili's description), we see that $V \cong V_G$. Furthermore, it is not hard to see that the restriction of G to ∂V can be made to agree with the restriction of H by matching them fiberwise, as required. \square

Then for each anti-Lefschetz critical point p , we replace H on a neighborhood of p with the local covering G . As noted above, all new vanishing cycles

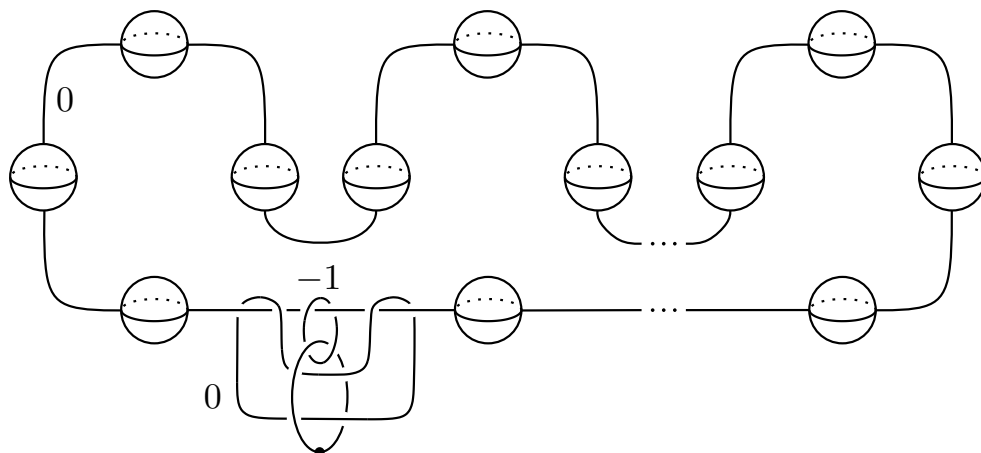


Figure 5.11: Neighborhood of $F \subset X$ with an extra 2-handle and round 1-handle added

introduced are non-separating, and all fibers are still connected. Furthermore, we can push the boundary of the new cap over any Lefschetz or anti-Lefschetz critical points, so that its image is parallel with the boundary of the base D^2 . Repeating this procedure for each anti-Lefschetz critical point yields the required broken Lefschetz fibration. \square

Now suppose that X is an oriented closed 4-manifold, and that $F \subset X$ is an embedded surface with $[F]^2 = 0$.

Proof of Theorem 1.4.4. We first build a concave broken fibration on a neighborhood of $F \subset X$, with no Lefschetz or anti-Lefschetz critical points. Starting with the standard $2g$ 1-handle diagram of $\nu F \cong F \times D^2$, where g is the genus of F , this could be accomplished by adding canceling handle pairs as in Example 4.6.2. Notice, however, that the induced open book on the boundary would then have disconnected binding, which would prevent us from applying Theorem 1.4.3.

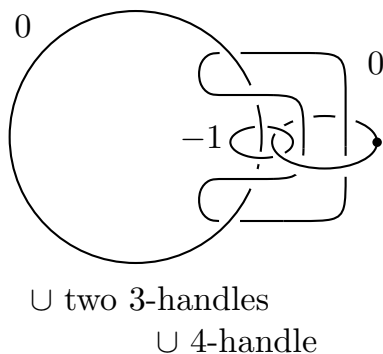


Figure 5.12: Handlebody structure of a neighborhood of S^2 in S^4

We thus instead think of the lone canceling 3-handle as being attached as a 1-handle to $X \setminus \nu F$, and construct a concave fibration f_1 on $X_1 = \nu F \setminus \{3\text{-handle}\}$, whose boundary open book decomposition has connected page and binding (see Figure 5.11). Theorem 1.4.3 then gives a convex f_2 on the complement $X_2 = X \setminus X_1$, which matches f_1 along the boundary. Gluing f_1 and f_2 gives the desired fibration f , where Properties 1-4 all follow from the corresponding properties in Theorem 1.4.3.

In the case when there is an embedded sphere transversely intersecting F in a single point, we can start with the flat product fibration $\nu F \rightarrow D^2$, to which we attach a 2-handle embedded in X along a trivial section of the boundary. The desired branched covering can be constructed first along νF (fiberwise), and then extended along this 2-handle. A matching branched covering over the complement of $\nu F \cup \{2\text{-handle}\}$ is then constructed as in Section 5.2. \square

Example 5.3.2 (Broken Lefschetz fibration on S^4 via branched coverings). Consider the diagram of S^4 in Figure 5.12. As in Figure 4.5, the union of all 0,1, and 2-handles in this decomposition gives a neighborhood of an unknotted $S^2 \subset S^4$, together with an additional round 1-handle and (ordinary) 2-handle

attached. Call the union of these handles X_1 , and set $X_2 = S^4 \setminus X_1$. The open book decomposition on $\partial X_1 = \partial X_2$ induced by the concave fibration $f_1 : X_1 \rightarrow S^2$ from the above proof will have a punctured torus page with trivial monodromy (see [16]). Hence it can be represented by a 4-fold simple branched covering $h : \partial X_2 \rightarrow S^3$ with two trivial sheets, and whose branch locus in S^3 is the closure of the trivial 5-strand braid (h can be described fiberwise by adding a trivial sheet to the branched covering in Figure 5.1).

The branched covering h extends to a covering $H : X_2 \rightarrow D^4$, which is built by turning the handle decomposition from Figure 5.12 upside-down, and viewing X_2 as a 0-handle with two 1-handles attached. The 0-handle can be expressed as a 4-fold covering of D^4 branched over three properly embedded unknotted disks. For each 1-handle we extend this covering over, a properly embedded unknotted disk is added to the branch locus. Hence the branch locus B_H of H in $D^4 \cong D^2 \times D^2$ is isotopic to the braided surface $\{p_1, \dots, p_5\} \times D^2$, for some collection of disjoint points $\{p_1, \dots, p_5\} \subset D^2$. The only critical points in the resulting broken Lefschetz fibration $f : S^4 \rightarrow S^2$ will thus lie along round 1-handle singularity in X_1 , and we recover Auroux, Donaldson, and Katzarkov's example in [4].

Given an arbitrary closed 4-manifold X , the above procedure can be repeated by adding the diagram in Figure 5.12 to any handle diagram for X . Alternatively, instead of adding Figure 5.12 we could obtain a higher genus fibration by adding the diagram in Figure 5.11 (along with two 3-handles, and $2g$ 0-framed 2-handles to cancel the 1-handles). When $g > 0$, the monodromy of the induced boundary open book will not be trivial however (see [16]).

Bibliography

- [1] Selman Akbulut and ÇağrıKarakurt. Every 4-manifold is BLF. *J. Gökova Geom. Topol. GGT*, 2:83–106, 2008.
- [2] J.W. Alexander. A lemma on systems of knotted curves. *Proc. Nat. Acad. Sci. USA*, 9(2):93–95, 1923.
- [3] Nikos Apostolakis, Riccardo Piergallini, and Daniele Zuddas. Lefschetz fibrations over the disk. *Preprint*, 2013. arXiv:1104.4536v3.
- [4] Denis Auroux, Simon K. Donaldson, and Ludmil Katzarkov. Singular Lefschetz pencils. *Geom. Topol.*, 9:1043–1114, 2005.
- [5] R. İnanç Baykur. Existence of broken Lefschetz fibrations. *Int. Math. Res. Not. IMRN*, pages Art. ID rnn 101, 15, 2008.
- [6] Refik İnanç Baykur. Topology of broken Lefschetz fibrations and near-symplectic four-manifolds. *Pacific J. Math.*, 240(2):201–230, 2009.
- [7] Israel Berstein and Allan L. Edmonds. On the construction of branched coverings of low-dimensional manifolds. *Trans. Amer. Math. Soc.*, 247:87–124, 1979.
- [8] Gerhard Burde and Heiner Zieschang. *Knots*, volume 5 of *de Gruyter Studies in Mathematics*. Walter de Gruyter & Co., Berlin, 1985.
- [9] Scott Carter, Seiichi Kamada, and Masahico Saito. *Surfaces in 4-space*, volume 142 of *Encyclopaedia of Mathematical Sciences*. Springer-Verlag, Berlin, 2004. Low-Dimensional Topology, III.
- [10] S. K. Donaldson. Lefschetz fibrations in symplectic geometry. In *Proceedings of the International Congress of Mathematicians, Vol. II (Berlin, 1998)*, number Extra Vol. II, pages 309–314, 1998.
- [11] Allan L. Edmonds. Extending a branched covering over a handle. *Pacific J. Math.*, 79(2):363–369, 1978.

- [12] Y. Eliashberg. Classification of overtwisted contact structures on 3-manifolds. *Invent. Math.*, 98(3):623–637, 1989.
- [13] John B. Etnyre and Terry Fuller. Realizing 4-manifolds as achiral Lefschetz fibrations. *Int. Math. Res. Not.*, pages Art. ID 70272, 21, 2006.
- [14] P. Freyd, D. Yetter, J. Hoste, W. B. R. Lickorish, K. Millett, and A. Ocneanu. A new polynomial invariant of knots and links. *Bull. Amer. Math. Soc. (N.S.)*, 12(2):239–246, 1985.
- [15] Terry Fuller. Hyperelliptic Lefschetz fibrations and branched covering spaces. *Pacific J. Math.*, 196(2):369–393, 2000.
- [16] David T. Gay and Robion Kirby. Constructing Lefschetz-type fibrations on four-manifolds. *Geom. Topol.*, 11:2075–2115, 2007.
- [17] Emmanuel Giroux. Géométrie de contact: de la dimension trois vers les dimensions supérieures. In *Proceedings of the International Congress of Mathematicians, Vol. II (Beijing, 2002)*, pages 405–414, Beijing, 2002. Higher Ed. Press.
- [18] Robert E. Gompf and András I. Stipsicz. *4-manifolds and Kirby calculus*, volume 20 of *Graduate Studies in Mathematics*. American Mathematical Society, Providence, RI, 1999.
- [19] John Lester Harer. *PENCILS OF CURVES ON 4-MANIFOLDS*. ProQuest LLC, Ann Arbor, MI, 1979. Thesis (Ph.D.)—University of California, Berkeley.
- [20] Kenta Hayano and Masatoshi Sato. Four-manifolds admitting hyperelliptic broken Lefschetz fibrations. *Michigan Math. J.*, 62(2):323–351, 2013.
- [21] Hugh M. Hilden. Three-fold branched coverings of S^3 . *Amer. J. Math.*, 98(4):989–997, 1976.
- [22] Ko Honda. Transversality theorems for harmonic forms. *Rocky Mountain J. Math.*, 34(2):629–664, 2004.
- [23] Mark Hughes. A note on Khovanov-Rozansky sl_2 -homology and ordinary Khovanov homology. *Preprint*, 2013. arXiv:1302.0331.
- [24] Magnus Jacobsson. An invariant of link cobordisms from Khovanov homology. *Algebr. Geom. Topol.*, 4:1211–1251 (electronic), 2004.

- [25] Vaughan F. R. Jones. A polynomial invariant for knots via von Neumann algebras [MR0766964 (86e:57006)]. In *Fields Medallists' lectures*, volume 5 of *World Sci. Ser. 20th Century Math.*, pages 448–458. World Sci. Publ., River Edge, NJ, 1997.
- [26] Seiichi Kamada. 2-dimensional braids and chart descriptions. In *Topics in knot theory (Erzurum, 1992)*, volume 399 of *NATO Adv. Sci. Inst. Ser. C Math. Phys. Sci.*, pages 277–287. Kluwer Acad. Publ., Dordrecht, 1993.
- [27] Seiichi Kamada. Alexander's and Markov's theorems in dimension four. *Bull. Amer. Math. Soc. (N.S.)*, 31(1):64–67, 1994.
- [28] Seiichi Kamada. On braid monodromies of non-simple braided surfaces. *Math. Proc. Cambridge Philos. Soc.*, 120(2):237–245, 1996.
- [29] Seiichi Kamada. Arrangement of Markov moves for 2-dimensional braids. In *Low-dimensional topology (Funchal, 1998)*, volume 233 of *Contemp. Math.*, pages 197–213. Amer. Math. Soc., Providence, RI, 1999.
- [30] Seiichi Kamada. *Braid and knot theory in dimension four*. Mathematical surveys and monographs. American Mathematical Society, 2002.
- [31] Mikhail Khovanov. A categorification of the Jones polynomial. *Duke Math. J.*, 101(3):359–426, 2000.
- [32] Mikhail Khovanov and Lev Rozansky. Matrix factorizations and link homology. *Fund. Math.*, 199(1):1–91, 2008.
- [33] Mikhail Khovanov and Lev Rozansky. Matrix factorizations and link homology. II. *Geom. Topol.*, 12(3):1387–1425, 2008.
- [34] Catherine Labruère and Luis Paris. Presentations for the punctured mapping class groups in terms of Artin groups. *Algebr. Geom. Topol.*, 1:73–114 (electronic), 2001.
- [35] Yanki Lekili. Wrinkled fibrations on near-symplectic manifolds. *Geom. Topol.*, 13(1):277–318, 2009. Appendix B by R. İnanç Baykur.
- [36] Andrea Loi and Riccardo Piergallini. Compact Stein surfaces with boundary as branched covers of B^4 . *Invent. Math.*, 143(2):325–348, 2001.
- [37] José María Montesinos. A note on moves and on irregular coverings of S^4 . In *Combinatorial methods in topology and algebraic geometry (Rochester, N.Y., 1982)*, volume 44 of *Contemp. Math.*, pages 345–349. Amer. Math. Soc., Providence, RI, 1985.

- [38] H. R. Morton. An irreducible 4-string braid with unknotted closure. *Math. Proc. Cambridge Philos. Soc.*, 93(2):259–261, 1983.
- [39] H. R. Morton. Threading knot diagrams. *Math. Proc. Cambridge Philos. Soc.*, 99(2):247–260, 1986.
- [40] R. Piergallini. Four-manifolds as 4-fold branched covers of S^4 . *Topology*, 34(3):497–508, 1995.
- [41] Lee Rudolph. Braided surfaces and Seifert ribbons for closed braids. *Comment. Math. Helv.*, 58(1):1–37, 1983.
- [42] Lee Rudolph. Special positions for surfaces bounded by closed braids. *Rev. Mat. Iberoamericana*, 1(3):93–133, 1985.
- [43] Lee Rudolph. Quasipositivity as an obstruction to sliceness. *Bull. Amer. Math. Soc. (N.S.)*, 29(1):51–59, 1993.
- [44] Lee Rudolph. Knot theory of complex plane curves. In *Handbook of knot theory*, pages 349–427. Elsevier B. V., Amsterdam, 2005.
- [45] Bernd Siebert and Gang Tian. On hyperelliptic C^∞ -Lefschetz fibrations of four-manifolds. *Commun. Contemp. Math.*, 1(2):255–280, 1999.
- [46] O. Ya. Viro. Lecture given at Osaka City University, September 1990.
- [47] E. C. Zeeman. Twisting spun knots. *Trans. Amer. Math. Soc.*, 115:471–495, 1965.